Republic of Iraq
Ministry of Higher Education & Scientific Research
University of Babylon
College of Education for Pure Sciences
Department of Physics

Influence of Nano Silicon Nitride on Structural, Optical, and Electrical Properties of Polymer Blend and it's Applications

A Thesis

Submitted to the Council of the College of Education for Pure Sciences, University of Babylon in Partial Fulfillment of the Requirements for the Degree of Master in Education / Physics

By

Ghaith Ahmed Abdullah Murad

B.Sc. of Science in Physics
University of Babylon/Department of Physics (2020)

Supervised by

Dr. Ahmed Hashim Mohaisen

2023 A.D. **1444 A.H.**

بسم الله الرحمن الرحيم

اقرأ باسم ربك الذي خلق ﴿1﴾

خلق الإنسان من علق ﴿2﴾

اقرأ وربك الأكرم ﴿3﴾ الذي علم بالقلم ﴿4﴾

علم الإنسان ما لم يعلم ﴿5﴾

صدق الله العظيم

سورة العلق

الآيات (1-5)

Dedication

To the Great Prophet "Mohammad"

To my the Prince of Believers, "Imam Ali"

To who gave me the endurance to complete my road my father

To the best woman in the universe my mother

To my supervisor

Dr. Ahmed Hashim

And

Everyone who has helped me ….

Ghaith …

Acknowledgments

In the Name of Allah, the Compassionate, the Merciful
First, thanks to Allah, the Lord of earth and heaven, for completing my research.
Special thanks to the Deanery of the College of Education for Pure Science, University of Babylon and the Department of Physics for offering me the opportunity to complete my research.
Then, I would like to express my thanks and appreciation to all of.....
Dear Supervisors Dr. Ahmed Hashim for his kindness in supervising this study and for all the effort he made.
To my family, who helped me reach this stage of study.
the respected discussion committee. To
And to everyone who helped me in my study and encouraged me even with a word.

Ghaith ...

Summary

The nanocomposites [Poly (methyl methacrylate) (PMMA)- Polyethylene glycol (PEG)/ Silicon nitride (Si_3N_4)] were prepared by casting method. To study antibacterial and gamma-ray shielding applications. The structural properties studied include Optical Microscope (OM), Fourier Transforms Infra-Red (FT-IR), and scanning Electron Microscope (SEM). The structure, optical and electrical properties of nanocomposites were studied. The optical microscopy images showed that with increasing concentrations of nanoparticles, network paths are formed inside the polymeric matrix that act as charge carriers. The SEM measurement results showed a good distribution and homogeneity in surface morphology.

The results of FT-IR indicate a physical interference between the polymer matrix and nanoparticles. The results of (PMMA-PEG/Si_3N_4) nanocomposite showed optical properties that the absorption coefficient, absorbance, refractive index, extinction coefficient, real and imaginary dielectric constants, as well as optical conductivity increases with increasing in the concentrations of Si_3N_4 NPs, while transmittance and energy gap decrease with increasing concentrations of nanoparticles. It also indicated that the highest absorption of spectrum happened in U.V region.

The results of the electrical properties of nanocomposites showed that the dielectric constant and dielectric loss increase with increasing concentrations of nanoparticles and decrease when the frequency of applied electric field increasing. while the A.C electrical conductivity increases with increang the frequency and weight concentrations of (Si_3N_4) NPs. The results of applications of (PMMA-PEG/Si_3N_4) nanocomposites against bacteria showed that the inhibition diameter

zone increases with increasing concentrations of nanoparticles, and the attenuation coefficients increase with the increase of nanoparticle concentrations, this is due to the absorption or reflection of gamma radiation by nanocomposite shielding materials. The (PMMA-PEG/Si_3N_4) nanocomposites have the highest attenuation coefficients.

Contents

No	Title	Page
	Dedication	I
	Acknowledgments	II
	Summary	III
	Contents	V
	List of Figures	IX
	List of Tables	XIII
	List of Abbreviations	XIII
	List of Symbols	XIV
	Chapter One: Introduction and Literature Reviews	1-19
1.1	Introduction	1
1.2	Polymer Blends	2
1.3	Classification of polymers	4
1.3.1	Classification of polymers based on source	4
1.3.2	Classification Based on the Structure of the Polymers	4
1.3.3	Classification of polymers based on homogeneity	5
1.4	Nanocomposites and their Applications	5
1.5	Nanomedicines	6
1.6	polymethylmethacrylate (PMMA)	8

1.7	**Polyethylene glycol (PEG)**	**10**
1.8	**Silicon nitride (Si_3N_4)**	**12**
1.9	**Literature Review**	**14**
1.10	**The Aim of Study**	**19**
Chapter Two: Theoretical Part		**20-33**
2.1	**Introduction**	**20**
2.2	**The Structural Properties**	**20**
2.2.1	**Optical Microscope**	**20**
2.2.2	**Fourier Transforms Infrared (FT-IR) Spectroscopy**	**21**
2.3	**The Optical Properties**	**22**
2.3.1	**Absorbance (A) and Transmittance (T)**	**23**
2.3.2	**The electronic transitions**	**23**
2.3.3	**Optical Constants**	**26**
2.3.4	**Optical conductivity**	**28**
2.4	**Electrical Properties**	**28**
2.4.1	**The A.C electrical conductivity**	**29**
2.5	**Anti-bacterial Application**	**30**
2.5.1	**The antibacterial mechanisms of nanomaterial**	**31**
2.6	**Gamma-ray shielding application**	**32**
Chapter Three: Practical Part		**34-41**
3.1	**Introduction**	**34**

3.2	The Materials Used in this Work	34
3.2.1	Matrix Material	34
3.2.1.1	Poly (methyl methacrylate) PMMA	34
3.2.1.2	polyethylene Glycol (PEG)	35
3.2.2	Additive Material	35
3.3	Preparation of (PMMA-PEG-Si_3N_4) Nanocomposites	36
3.4	Measurements of Structural Properties for Nanocomposites	37
3.4.1	Optical Microscope (OM)	37
3.4.2	FTIR spectrometer	38
3.4.3	Scanning Electron Microscope (SEM)	39
3.5	Measurements of Optical Properties for Nanocomposites	39
3.6	Measurements of A.C Electrical Conductivity Properties for (PMMA-PEG-Si3N4) Nanocomposites	40
3.7	Measurements of Anti-bacterial Activity for Nanocomposites	40
3.8	Gamma Ray Shielding Application Measurements of Nanocomposites	41
	Chapter Four: Results, Discussion	**42-63**
4.1	Introduction	42
4.2	Structural Properties of (PMMA-PEG/Si_3N_4) nanocomposites	42
4.2.1	Optical Microscope (OM) and Scanning Electronic Microscope (SEM) of (PMMA-PEG-Si_3N_4)	42
4.2.2	Fourier Transform Infrared Radiation (FTIR) of (PMMA-PEG/Si_3N_4) Nanocomposites	45
4.3	The Results of Optical Properties	47
4.3.1	Absorbance and transmittance of (PMMA-PEG/Si_3N_4) nanocomposites	47

4.3.2	**Absorption coefficient (α) of (PMMA-PEG/Si_3N_4) nanocomposites**	**49**
4.3.3	**Extinction coefficient (k) of (PMMA-PEG/Si_3N_4) nanocomposites**	**50**
4.3.4	**Refractive index (n) of (PMMA-PEG/Si_3N_4) nanocomposites**	**51**
4.3.5	**Energy gap of (PMMA-PEG/Si_3N_4) nanocomposites**	**52**
4.3.6	**The Real and imaginary parts of dielectric constant (ε1 and ε2)**	**54**
3.3.7	**Optical conductivity (σ) of (PMMA- PEG/Si_3N_4) nanocomposites**	**56**
4.4	**The Results of A.C Electrical Properties**	**57**
4.4.1	**Dielectric constant (ε') and dielectric loss (ε'') of (PMMA-PEG/Si_3N_4) Nanocomposites**	**57**
4.4.2	**A.C Electrical conductivity of (PMMA-PEG/Si_3N_4) nanocomposites**	**61**
4.5	**Application of (PMMA-PEG/Si_3N_4) Nanocomposites for Antibacterial Activity**	**62**
4.6	**Application of (PMMA-PEG/Si_3N_4) Nanocomposites for Gamma Ray Shielding**	**66**
4.7	**Conclusions**	**68**
4.8	**Future Works**	**69**
	The References	**70**

List of Figures		
No.	Figure	Page
1.1	Nanoparticles-based targeted drug delivery	8
1.2	Molecular formula of PMMA	9
1.3	The chemical structure of PEG	11
2.1	(a) Optical microscopy, (b) SEM Quanta device	21
2.2	Basic component in Fourier transform infrared spectrometer	22
2.3	Types of electronic transfers	25
3.1	poly (methyl methacrylate) Polymer	34
3.2	Polyethylene glycol Polymer	35
3.3	Silicon nitride	36
3.4	The outline represents the practical part	37
3.5	Optical Microscope used in the work	38
3.6	Fourier transform infrared spectroscopy device used in the work	38
3.7	UV–Visible Spectrophotometer (Shimadzu-1800)	39
3.8	Diagram for system of A.C electrical measurement system	40
3.9	Gamma-ray shielding	41
4.1	The optical microscope image (X10) for (PMMA-PEGSi_3N_4)	43

	nanocomposites:(A) for blend, (B) 1.6 wt.%, (C) 3.2 wt.%,(D) 4.8 wt.% , and (E) 6.4 wt.%	
4.2	The images of (SEM) for (PMMA-PEG-Si_3N_4) nanocomposites A for blend, B. 1.6 wt.%, (C) 3.2 wt.%, (D) 4.8 wt.% and (E) 6.4 wt.%	44
4.3	FT-IR spectra (PMMA-PEG/Si_3N_4) nanocomposites: (A) for blend, (B) 1.6 wt.% ,(C) 3.2 wt.%,(D) 4.8 wt.% and (E) 6.4 wt.%	46
4.4	Variation of absorbance for (PMM-APEG /Si_3N_4) nanocomposites with Wavelength	48
4.5	Variation of transmittance for (PMMA-PEG/Si_3N_4) nanocomposites with wavelength	48
4.6	Variation of absorbance coefficient (α) for (PMMA-PEG/Si_3N_4) nanocomposites with photon energy	50
4.7	Variation of extinction coefficient for (PMMA-PEG/Si_3N_4) nanocomposites with wavelength	51
4.8	Variation of refractive index for (PMMA-PEG/Si_3N_4) nanocomposites with wavelength	52
4.9	Variation of $(\alpha h\nu)^{1/2}$ for (PMMA-PEG/Si_3N_4) nanocomposites with E_{ph}	53
4.10	Variation of $(\alpha h\upsilon)^{1/3}$ for (PMMA-PEG/Si_3N_4) nanocomposites with E_{ph}	54
4.11	Performance of real part of dielectric constant for (PMMA-PEG/Si_3N_4) nanocomposites with wavelength	55

4.12	Performance of imaginary part of dielectric constant for (PMMA-PEG/Si_3N_4) nanocomposites with wavelength	56
4.13	Variation of optical conductivity for (PMMA-PEG/Si_3N_4) nanocomposites with wavelength	57
4.14	Performance of dielectric constant for nanocomposites against frequency	58
4.15	Performance of dielectric loss for nanocomposites against frequency	59
4.16	Performance of dielectric constant for (PMMA-PEG) blend with the concentration of (Si_3N_4) nanoparticles	60
4.17	Performance of dielectric loss for nanocomposites concentrations of (Si_3N_4) nanocomposites	60
4.18	Performance of A.C conductivity of (PMMA-PEG/Si_3N_4) Nanocomposites with frequency.	61
4.19	Performance of A.C conductivity for (PMMA-PEG) blend with concentrations of (Si_3N_4) nanoparticles	62
4.20	Images of inhibition zone for Staphylococcus	63
4.21	Images of inhibition zone for Escherichia coli	64
4.22	Inhibition zone diameter of (PMMA-PEG/Si_3N_4)	65

	nanocomposites against Staphylococcus bacterial	
4.23	Inhibition zone diameter of (PMMA-PEG/Si_3N_4) nanocomposites against Escherichia coli	65
4.24	Variation of (N/N_0) for (PMMA-PEG/Si_3N_4) nanocomposite	66
4.25	Variation of attenuation coefficients of gamma radiation for (PMMA-PEG/Si_3N_4) nanocomposites	67

List of table

No.	Table	Page
1.1	Important properties of PMMA polymer	10
1.2	The most important physical properties of PEG polymer	12
1.3	Physical and mechanical properties of Si_3N_4	13
4.1	inhibition zone diameter of (PMMA-PEG/Si_3N_4) nanocomposites	64

Symbol	Physical terms
A.C	Alternating current
C.B	Conductive Band
E. coli	Escherichia coli bacteria
FTIR	Fourier Transform Infrared Radiation
NPs	Nanoparticles
OM	Optical Microscope
PMMA	Poly (methyl methacrylate) polymer
PEG	Polyethylene glycol
ROS	Reaction oxygen species
Si_3N_4	Silicon nitride
S. aureus	Staphylococcus aureus bacteria
SEM	Scanning Electron Microscope
UV	Ultraviolet
V.B	Valence Band

List of symbol	
Symbol	Physical terms
A	Absorbance
a	the area of the capacitance plate
B	Constant Depended on Type of Material
C	Capacitance
c	Velocity of light
C_o	Vacuum Capacitor
C_p	Parallel Capacitance
D	Dispersion Factor
E_g	Energy Gap
E_g^{opt}	Optical Energy gap
E^{ph}	Phonon Energy
h	Plank constant
I	Instantaneous photon intensity
I_A	Absorbed Light Intensity
I_o	Incident Intensity of light

$\mathbf{I_T}$	Intensity of transmittance ray
j	Imaginary number
K	Wave Vector
k	Extinction Coefficient
N	Number of particles counted over
$\mathbf{N_O}$	Number of radiation particles counted over
n	Refractive index
R	Reflectance
r	Exponential constant
T	Transmittance
x	Thickness
α	Absorption coefficient
$\mathcal{E}$	Complex dielectric constant
$\mathcal{E}_1$	Real dielectric constant
$\mathcal{E}_2$	Imaginary dielectric constant
$\mathcal{E}^*$	Complex permittivity
$\mathcal{E}_o$	Vacuum permittivity
$\mathcal{E}'$	Dielectric constant

ε "	Dielectric loss
ω	Angular frequency
$\sigma_{A.C}$	Alternating Conductivity
σ_{opt}	Optical conductivity
ν	Frequency
λ	Wavelength
Δ**Sm**	Change in entropy
Δ**Gm**	Change in free energy
Δ**Hm**	Change in enthalpy
μ	The attenuation coefficient\

Chapter one

Introduction and Literature Review

1.1 Introduction

Polymer science is a relatively new discipline which deals with plastics, natural and synthetic fibers, rubbers, coatings, adhesives, sealants, etc [1]. Polymers have a large molecular weight and are composed of a higher number of repeating units. Polymer synthesis takes place on a very wide scale and polymers have a large range of properties to use in different applications[2]. polymers are produced from monomers through polymerization. Through chemical reactions, monomers form together two types of chains. One is a linear chain and the other is a three - dimensional chain. Polymers have three - dimensional chains[3]. Tens, hundreds, or even thousands of monomer units can be found in polymer molecules. The most important characteristics of polymer composites are their ease of formation, low density in comparison to metals, superior surface quality, and increased corrosion resistance.

Polymer composites can compete with metals in terms of durability and hardness, in addition to many advantages such as high strength, size, and thermal stability, hardness, and abrasion resistance. Aside from all of these advantages, the lightness of polymer composite materials gives them an advantage in many areas. Because of their intriguing properties and potential, polymer composite-based materials have piqued the interest of scientists and active multidisciplinary and industrial research group[4].

Polymers are classified as either natural that resulted from natural biosynthesis, or synthetic[5]. Advancement in polymer science has brought new applications of polymers or plastics in our daily lives[6]. Due to their chemical stability, versatility, lightness, and limited cost with respect to other classes of materials (i.e.

metals and ceramics), in the last decades, polymers have found a widespread application in many technological fields, such as construction, electronics, packaging, and health care[7].

Polymer nanocomposites are a promising type of polymeric material that can be used instead of conventional polymers and other materials. It has been discovered in recent decades that adding small amounts of nanofillers to polymers can increase their thermal, mechanical, barrier, and flammable properties compared to conventional polymers and it is one of the low-cost and easy methods to modify the structure of polymers[8]. Currently, polymer composites are of high interest in different energy applications because of their pliable characteristics and their easy-to-use[9]. these embedded particles within the polymer matrix also impact the physical properties of the host. Polymer ceramic hybrid composites, in particular, are promising functional materials in a variety of disciplines, demonstrating useful optical, electrical, thermal, mechanical, and antibacterial characteristics [10].

1.2 Polymer Blend

The polymer blend definition of polymeric mixtures as a combination of two or more polymers are polymeric mixtures preparation process mediated by blending polymers in the liquid state or in the solid state or in the molten phase[11],In addition, the high prices of some polymers and some of their limitations are other factors that have led to research on alternatives such as polymer blends[12] Polymer blending is a convenient route for the development of new polymeric materials, which combine the excellent properties of more than one existing polymer. This strategy is usually cheaper and less time-consuming than the development of new monomers and/or new polymerization routes, as the basis for

entirely new polymeric materials[13]. polymer blends are widely used in many pharmaceutical and medical applications including drug delivery system, bone repair, enzyme immobilization, wound dressing, they play an important role as a temporary scaffold and temporary barrier[14]. The most important relationship governing mixtures of dissimilar components is:

$\Delta Gm=\Delta Hm - T\Delta sm$ ..... (1.1)

where ΔGm is the free energy of mixing.

ΔHm is the enthalpy of mixing (heat of mixing).

ΔSm is the entropy of mixing.

For miscibility to occur, ΔGm must be smaller than (0) [15]. This approach has not been without its difficulties and has not developed as rapidly as it might have, in part because most physical blends of different high molecular weight polymers prove to be immiscible. That is, when mixed together, the blend components are likely to separate into phases containing predominantly their own kind[16]. Forming polymer blends is a traditional method for making new materials with enhanced properties. Unfortunately, because of the large unfavorable enthalpy, most polymer blends tend to phase separate, which results in poor mechanical properties. Therefore, controlling the phase behavior and morphology becomes a key factor in determining the performance of polymer blends, which mainly rely on the interface between polymer components[17].

1.3 Classification of polymers

Polymers cannot be classified under one category because of their complex structures, different behaviors and vast applications. We can, therefore, classify polymers based on the following considerations.

1.3.1Classification of polymers based on source

Polymers may be divided into two types[18]:

a. Natural polymer: It generally consists of proteins, carbohydrates, cellulose and rubber found in plants and animals, which primarily serve as structural support.

b. Synthetic polymer: Which constitutes the great majority of industrially necessary polymers including rubber, plastics, and synthetic leather, is created from straightforward chemical components. Other qualities offered by synthetic polymers include thermal stability, mechanical, and physical characteristics

1.3.2 Classification Based on the Structure of the Polymers:

There are three different types based on the structure:

1.Linear polymers: these polymers are linearly organized. Only a bifunctional monomer can form linear polymers. They are usually thermoplastic polymers and, except for very high molecular weight materials, are soluble in solvents. These polymers have the ability to crystallize more than other polymers[19].

2.Branched Polymers: The reaction between polyfunctional molecules results in structural units that can be connected in such a way as to form non-linear structures. In certain situations, the side growth of each polymer chain can be

stopped before the chain has a chance to link up with another chain. The resulting polymer molecules are said to be bundled. Branching can produce several physical properties in a polymer, such as a decrease in solvent solubility, a rise in the softening point and also a decrease in thermoplastic properties[20].

1.3.3 Classification of polymers based on homogeneity

Polymers are classified based on the homogeneity of the repeater units to: **a. Homo polymers:** Polymers made from a single monomer species called the homo polymer , example for this is polyvinyl chloride(PVC)(monomer is vinyl chloride)[21].

b. Copolymers: Copolymers are made up of two units of duplicating units of different monomers. It is classified as random, alternative, block, and graft copolymers. An example of this is polyethene-vinyl acetate (PEVA)[22].

c. Composite polymers: It is The process of modifying the characteristics of homogenous polymers by including new materials and formulas[23].

1.4 Nanocomposites and their Applications

Nanocomposites are a combination of two or more phases containing different compositions or structures, where at least one of the phases is in the nanoscale regime. These materials exhibit behavior different from conventional composite materials with microscale structures[24]**,** which are one of the most important materials of modern technology, Composites are generally divided into three basic classes according to the size of the reinforcement in the structures. These are macro composites, micro composites, and nanocomposites[25]. nanocomposites

with $d<100$ nm, which represent a new generation of materials.The second group of materials exhibits new physical, functional and service properties[26]. The size-induced properties of nanoparticles enable the development of new applications or the addition of flexibility to existing systems in many areas, such as catalysis, optics, microelectronics, and so on[27].Nanotechnology is defined as the understanding and control of matter at dimensions between 1 and100 nm where unique phenomena enable novel applications[28].Nanotechnology encompasses the nanomanufacturing, nanomaterials, and application of physical, chemical, and biological systems at scales ranging from individual atoms or molecules to submicron dimensions, as well as the integration of the resulting nanostructures into larger systems. It spans scientific fields, including chemistry, physics, material science, engineering, and manufacturing[29] Some of the potential applications of nanotechnology are as follows[30].

- Antibacterial dressings and coatings
- Micro sensors and diagnostics for more effective treatment
- Barriers for thermal and optical applications
- Miniature thin film photovoltaic solar cells for cost effective power generation for applications ranging from laptop to automobiles

1.5 Nanomedicines

A new era of nanomedicine that uses devices of nanoscale size to address urgent needs for improved diagnosis and therapy of diseases is being etched in the 21st-century[31]. Targeted drug delivery is one of the greatest challenges in medicine [32]. Drugs are conventionally administered in the patient orally in capsule or liquid forms. However, this approach is not always effective in targeting specific cells for treatment, diagnosis, or imaging[33].The field of nanomedicine

aims to use the properties and physical characteristics of nanomaterials for the diagnosis and treatment of diseases at the molecular level[34].Nanoparticles have the potential to revolutionize is a medicine; nanomedicine could provide new technological advances in not only developing new and novel drugs but also reformulation of already existing drugs to increase their efficacy, improve delivery and lower side effects [35]. To date, various nanomedicines have been developed and commercially applied in clinical and non-clinical areas. Nano medicines have shown essential characteristics such as efficient transport through fine capillary blood vessels and lymphatic endothelium, longer circulation duration and blood concentration, higher binding capacity to biomolecules (e.g. endogenous compounds including proteins). These characteristics differ from those of conventional medicines depending on physiochemical properties (e.g.; particle surface, size and chemical composition) of the nano-formulations[36]. Due to the nano size, they are normally composed of thousands of atoms with a high surface area so that a higher therapeutic payload (e.g.,radioactive isotopes or chemotherapy drugs) can be carried to or encapsulated in the nanostructure. Once delivered and recognized by a receptor, the high-dose therapeutic load can cause more devastating damage to cancer cells at the targeted site[37].

The long-term goal of nanomedicine research is to characterize quantitative molecular-scale components known as nanomachinery, as well as to precisely control and manipulate nanomachinery in cells to improve human health, understand the cellular mechanisms in living cells and develop advanced technologies for early diagnosis and treatment of various diseases[38].

The key objectives when designing NPs as a cargo system for carrying the pharmacological active agents is to avoid the clearance by the biological barriers

and to reach the impaired cells and delivering the drug at a therapeutically optimum rate with the appropriate dosage. Figure (1.1) shows nanoparticles based targeted drug delivery[39].

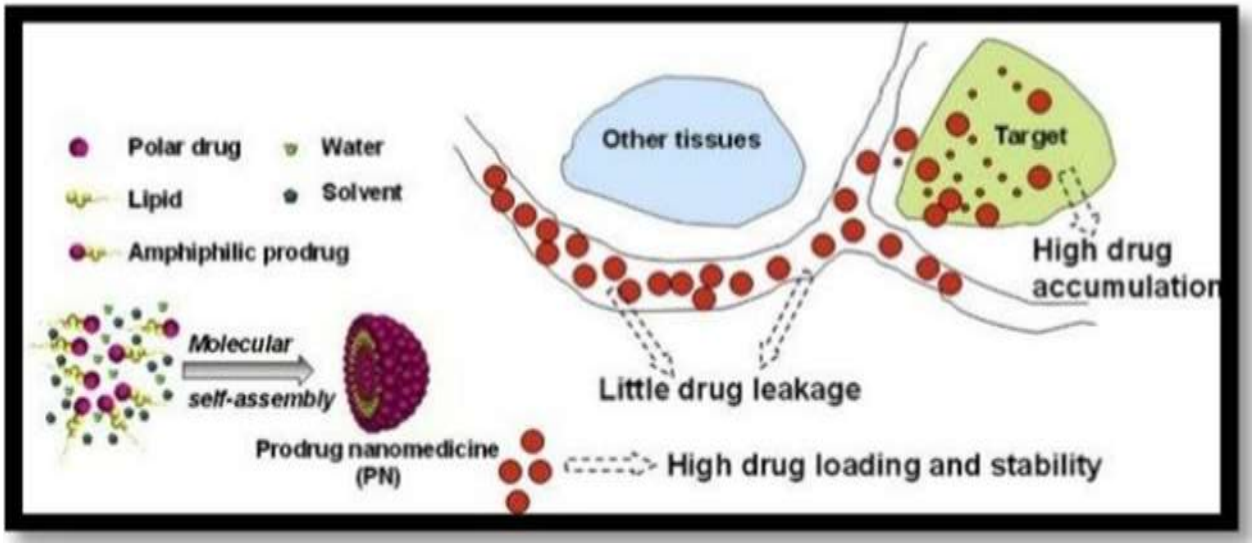

Figure (1.1). Nanoparticles based targeted drug delivery[39]

1.6 Polymethylmethacrylate (PMMA)

polymethylmethacrylate (PMMA) is a the linear thermoplastic polymer with the chemical formula $(C_5H8O_2)n$. It has a melting point equal to 160 C° and a glass transition the temperature of 115 C° [40]. PMMA exhibits excellent material properties such as exceptional mechanical strength, hardness, high rigidity, transparency, and good insulation properties [41]. Additionally, it possesses very good optical properties with a refractive index ranging between 1.3 and 1.7 .Owing to its high impact strength, lightweight, and shatter resistance, the PMMA is one of the best organic optical materials, and it is widely used as a substitute for inorganic glass[42]. poly methyl methacrylate (PMMA) is a polymer that is most commonly used in dental laboratories (to make orthodontic retainers and dentures and for repair), dental clinics(for relining dentures and temporary crowns), and industry (such as fabrication of artificial teeth) [43]. Polymethyl methacrylate is still being

used as base material or clip carrier material, but it is hard and heavy so acrylic resins are used for the fabrication of prosthetic eyes in ocular or orbital prostheses[44]. Figure (1.2) shows molecular formula of PMMA[45]. Table (1.1) shows important properties of PMMA polymer[46,47].

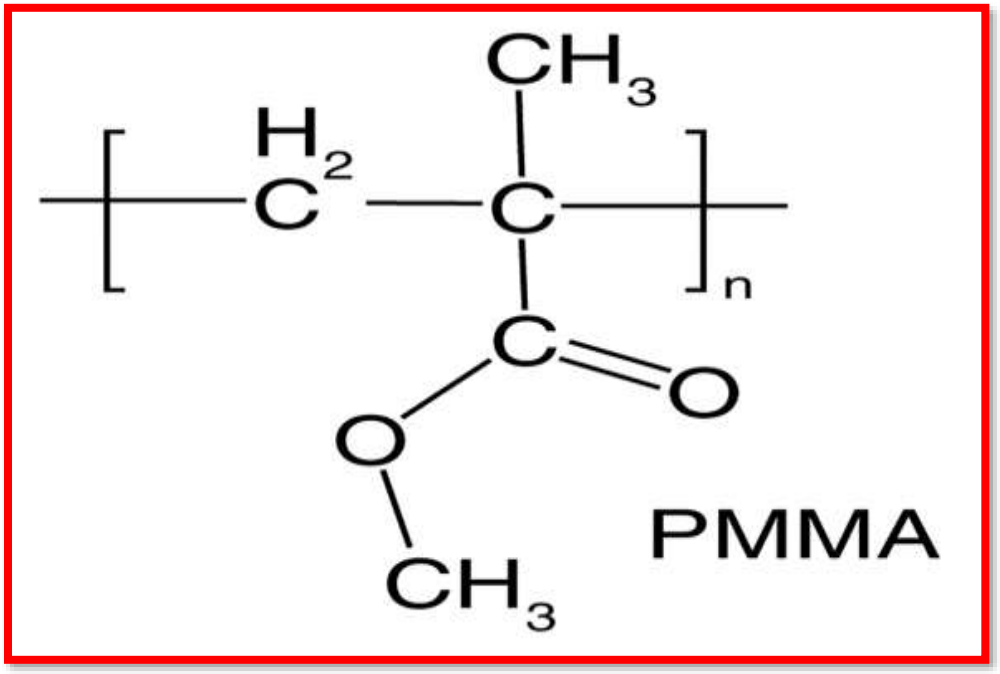

Figure (1.2). Molecular formula of PMMA[45]

Table (1.1): important properties of PMMA polymer[46,47]

Property	PMMA
Chemical formula	**CH2=C(CH3)COOH3**
Density (g/cm3)	**1.18**
Boiling point	**200C°**
Glass Transition Temp. (Tg) (C°)	**110 to 120**
Melting Point (C)	**220–240**
Water Absorption (%)	**0.3**
Surface Hardness (Rockwell)	**M92, M90-M100**

1.7 Polyethylene glycol (PEG)

The general formula H (OCH_2CH_2)n OH, where n is the average number of repeating oxyethylene groups and it is commonly found in many household products. Because of its low toxicity and low hazard risks, it is approved for use in different laxatives[48]. PEG earns it is important because of its high structure flexibility, biocompatibility, amphiphilicity, devoid of any steric hindrances, and high hydration capacity[49]. Polyethylene glycol (PEG) is a faculty of water soluble polymers with many different molecular weights that exhibits useful

properties such as protein resistance, low toxicity and immunogenicity [43], that is usually employed in many industries, including cloth, rubber, textiles, wood, metal, pharmaceuticals, coatings and cosmetics. PEG is also obtainable in different geometric shapes. Figure(1.3) gives the chemical structure of PEG[50]. Table (1.2) shows important physical properties of PEG polymer[51].

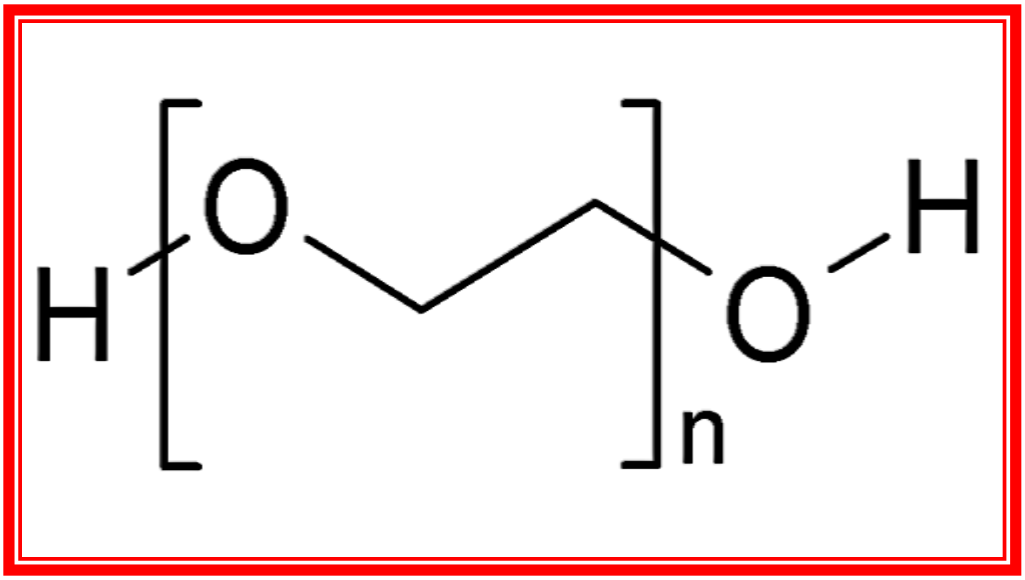

Figure (1.3). Part of the chemical structure of PEG[50]

Table (1.2): The most important physical properties of PEG polymer[51]

Properties	Description
Average Molecular Weight	**20000(g/mol)**
Flash point	**182–287 ◦C**
Appearance	**Clear liquid or white solid**
Density	**1.1–1.2**
Melting point	**54–58 C°**
Degradation temperature	**234 C°**
Toxicity	**Non-toxic and non-immunogenic**
Stability	**Stable under ordinary conditions of use and storage**
Odor	**Mild**

1.8 Silicon nitride (Si_3N_4)

Silicon nitride (Si_3N_4) is a nitrogen compound of highly covalent bond[52]. the bonding in Si_3N_4 can be estimated to be 70% covalent in character[53].Silicon nitride is a material of great technological interest due to its mechanical and electronic properties that make it suitable for several applications. Silicon nitride has high density, high melting temperature, low mechanical stress, and strong resistance against thermal shock. Due to its superior mechanical properties at high

temperatures, it has been considered as a prototypical material for uses in engine components and cutting tools. It has high dielectric constant [54], other engineering applications are also under consideration, such as (energy conversion) systems, industrial heat exchangers, as wear-resistant material in metals processing and as material for ball and roller bearings[55]. Si_3N_4 has also been considered as a material for nuclear fusion reactors in high-temperature gas-cooled reactors and very high-temperature reactors[56]. The wear resistance and chemical inertness of Si_3N_4 also make it useful as a protective coating for magnetic thin films in disk drives[57] .Table (1.3) shows physical and mechanical properties of Si_3N_4 [58].

Table (1.3): physical and mechanical properties of Si_3N_4[58].

Properties	Si_3N_4
Melting point (C°)	**1900**
Density (g cm^{-3})	**3.17–3.20**
Hardness (GPa)	**18**
Thermal Conductivity (Wm^{-1} K^{-1})	**10–162**
Fracture Toughness (MPa $m^{1/2}$)	**Crystal Structure**
Crystal Structure	**Hexagonal**

1.9 Literature Review

(B. H. Rabee *et al*.) in 2015 [59], prepared the composite of (PEG/PVA-Ag) with different weight percentages of Ag mamoparticels.The effect of addition of Ag on some optical properties of (PEG/PVA) was studied in the wavelengths (from200 to 1100) nm.The extinction coefficient, absorption coefficient, and energy gap of the indirect allowed and forbidden transition have been determined. Results showed that the extinction coefficient and absorption coefficient increase while the energy gap of the indirect allowed and forbidden transition decreases with the wight ratios of Ag.

(R. G. Kadhim) in 2015[60], studied the effect of adding TiO_2 nanoparticles on the electrical properties of the PMMA polymer. The samples were prepared by casting with weight ratios of TiO_2 (0,3,5,7) wt.%. The electrical insulation constant, electrical loss, and alternating electrical current conductivity of the nanocomposite (PMMA-TiO_2) increased with increasing nanoparticle concentrations (TiO_2). The dielectric constant and dielectric loss of the (PMMA-TiO_2) nanocomposite decrease as the frequency of the applied electric field increases, but the A.C electrical conductivity increases.

(B. H. Rabee and B. A. Al-Kareem) in 2016[61], studied the effect of adding copper oxide nanoparticles on the optical properties of polymethyl methacrylate. The samples were prepared by using the casting method. At wavelengths ranging from 300 to 1000 nm, the absorption spectra were recorded. They found that, as the concentration of copper oxide nanoparticles increases, the (absorption coefficient, extinction coefficient, refractive index, and real and imaginary dielectric constants) of (PMMA-CuO) nanocomposites increase. As the concentration of copper oxide

nanoparticles increase, the energy band gap of (PMMA-CuO) nanocomposites decreases.

(M. A. Habeeb) in 2016 [62], studied the effect of adding the nanoxide particles of yttrium on the electrical and optical properties of the (PVA-PAA-PEG) polymer blend . The results showed that as the concentration of yttrium oxide nanoparticles increased, the dielectric constant, dielectric loss, and A.C electrical conductivity increase. As frequency increases, the dielectric constant and dielectric loss decrease.

(H. M. Shanshool *et al*.) in 2016 [63], prepared four types of polymers (PMMA-PS-PVDF-PVA) that are used as polymer matrices, while different concentrations of ZnO nanoparticles are used as fillers. The UV-visible transmittance spectra showed low transmittance in the UV region, which is inversely proportional to ZnO nanoparticle concentration. The energy gap values in all samples decreased as the weight percentage of ZnO nanoparticles in nanocomposites increased.

(H. M. Mohssin) in 2017[64], investigated the effects of addition of Ag nanoparticles on optical properties of polyvinyl alcohol (PVA) and Polyethylene glycol (PEG-4000) blend. The results were showed that the optical constants increase as the concentration of silver nanoparticles increases. The energy gap shrank as the weight percentages of silver nanoparticles increased.

(I. R. Agoo *et al*.) in 2017[65], made (PVA–PEG–PVP–ZrO_2) nanocomposites. They found that, the conductivity of (PVA–PEG–PVP–ZrO_2) nanocomposites is increased with the increase of zirconium oxide nanoparticles concentration, and have higher attenuation coefficients for gamma radiation.

(S. Devikala *et al*.) in 2018[66], prepared the (PMMA/TiO_2) composites by using the sol-gel method. The composite samples were characterized by XRD, FTIR,

DSC and SEM. The addition of TiO_2 improved the composite's structural, morphological, and conductivity properties. The dielectric and A.C. conductivity of the samples increased with increasing TiO_2 concentration and temperature. The polymer composites created were suitable for a variety of technological applications.

(K. Kannan *et al.*) in 2018 [67], fabricated (PEG-PVP/Ag_2S) polymer nanocomposites by solvent casting. The vibrational nature of the bond presented in the prepared material was investigated using FTIR. The results showed that the SEM image confirms the sample's surface smoothness.

(M. H. Suhail) in 2019[68], prepared polymer films of (PEG-PVA) with different concentrations of $MnCl_2$ (0, 2, 4, 6, and 10 %wt.) using the casting technique. Absorption coefficient (α), refractive index (n), extinction coefficient (k_o), and the dielectric constants (real and imaginary parts) increase with increasing the concentration of $MnCl_2$.

(M. Bafna *et al*.) in 2019 [69], examined the optical parameters of (PMMA-K_2CrO_4). They added nanoparticles (K_2CrO_4) to the PMMA polymer in different weight ratios. The optical results showed the absorption coefficient, extinction index, refractive index, and real and imaginary of the dielectric constant improvement when potassium chromate was added.

(P. Rani et al) in 2020 [70], prepared polyvinyl alcohol (PVA) and polyethylene glycol (PEG) blend nanocomposite films reinforced with various loadings of carbon black nanoparticles (CBNPs). FTIR spectroscopy was used to investigate the structural properties of PVA/PEG/CBNPs nanocomposites, revealing a strong interaction of CBNPs with the polymer blend. The addition of CBNPs improved the dielectric properties.

(J. Q. M. Almarashi and M. H. Abdel-Kader) in 2020 [71]**,** synthesized (PVA/PEG-CuS) nanocomposite by using the casting technique. The optical transmittance revealed an apparent decrease (more than 40% for films doped with 5% CuS). Optical constants and dispersion parameters proved to be directly affected by nanoparticle concentrations. The optical energy gap values of polymer films decreased from 5.3 to 3.3 eV with the CuS nanoparticles' incorporation

(P. Dhatarwal *et al.*) in 2021 [72], studied the polymer nanocomposite (PNC) films comprising alumina (Al_2O_3) and silica (SiO_2) nanoparticles (1, 3, and 5 wt%) dispersed in poly(methyl methacrylate) (PMMA) matrix. The results showed that the UV-Vis absorbance, transmittance, and reflectance spectra of these PNCs changed gradually as the Al_2O_3 and SiO_2 content of the films increased. With increasing filler concentration, the energy bandgap decreases while refractive indices and optical conductivity improve.

(S. S. Al-Abbas *et al.*) in 2021[73], fabricated the polymer compounds (PEG-PVA-GO) with different molecular weights from PEG and PVA using developed mixing-sonication-solution methods. With the increasing frequency of the electric field, the effect of graphene oxide on the alternating electrical properties revealed a decrease in the dielectric constant and isolation loss of the polymer compounds (PVA-PEG-GO). It was also demonstrated that electrical conductivity increased. In addition to the contribution of GO, increasing the polymer molecular weight revealed an extraordinary improvement in the electrical properties, bringing promising and performance materials for electronic, photovoltaic devices, heterojunction, solar cells, and energy storage systems, among other significant applications

(Z. K. Heiba *et al*.) in 2022 [74], studied the optical parameters of polyvinyl alcohol/polyethylene glycol blend (PVA/PEG) and added Nano gadolinium oxide (Gd_2O_3). The results showed that the optical bandgap of the PVA/PEG blend was decreases, while the values of refractive index and extinction coefficient were enhanced as the amount of Gd_2O_3 increased in the blend

(F. S. Jaber *et al*.) In 2022 [75], designed the silicon nitride (Si_3N_4) and silicon bromide ($SiBr_4$) doped polyvinyl alcohol (PVA) as promising semiconductors materials which can be used in various electronics and optical fields. The results showed that the (PVA/Si_3N_4/$SiBr_4$) new structures have excellent optical and electronic properties. The (PVA/Si_3N_4/$SiBr_4$) structures have wide absorption spectra and an energy gap of about (0.35 eV) which makes it appropriate for various electronics and photonics fields.

1.10 The Aim of the work

The aim of this work can be summarized in the following points:

1. Preparation of (PMMA-PEG/Si_3N_4) which is a new nanocomposites to use in biomedical applications.
2. Studying the structural, dielectric and optical properties of (PMMA-PEG/Si_3N_4) nanocomposites.
3. Study the antibacterial activity and radiation shielding applications of (PMMA-PEG/Si_3N_4) nanocomposites.

Chapter Two

Theoretical Part

2.1 Introduction

This chapter includes a general description of the theoretical component, as well as physical concepts, scientific clarifications, relationships, and rules used to comprehend the findings.

2.2 The Structural Properties

2.2.1 Optical Microscope

Imaging is a valuable tool for determining the microstructure of materials. The characterization of a material necessitates measurements of the size and shape of material features, which are frequently accomplished using an automated image analysis method. As a result, image-based characterization of a material's microstructure can be viewed as a collaboration between the imaging system and the image analysis method. Some imaging modalities, such as optical microscopy (OM) and scanning electron microscopy (SEM), show the imaged sample's surface directly. In general, there are two types of microscopy: optical microscopy (OM) and scanning electron microscopy (SEM). For the last two centuries, OM has been used in the form of a simple device with limited capabilities. Unlike SEM, which is based on electron emission, the main principle of work in OM is light. Simple OM has one lens, whereas compound OM has two.

The lenses work by bending light to magnify images. The magnification of modern OM is 400–1000 times the original size, which is very low when compared to SEM, which has a magnification of 300,000x. OM can examine both living cells and solid materials. However, only a few small organics and solid pieces can be seen. This is due to the OM's ability to handle small and thin samples. SEM, on the other hand, provides a more detailed field with gray-scale images. As a result,

SEM is more expensive than OM and cannot be easily maintained. OM images display the true colors[76] . Figure (2.1) shows Optical microscopy, and SEM Quanta device.

Figure (2.1). (a) Optical microscopy, (b) SEM Quanta device [76]

2.2.2 Fourier Transforms Infrared (FT-IR) Spectroscopy

A spectrophotometer is an instrument that determines the absorption spectrum of a compound. When compared to a traditional spectrophotometer, a Fourier transform spectrophotometer provides the IR spectrum much faster. The main component of a simple FTIR spectrophotometer is depicted schematically in Fig. (2.2). The instrument generates an IR radiation beam from a glowing black-body source. Following that, the beam passes through an interferometer, where spectral encoding occurs. In an interferometer, the recombination of beams with different in path lengths produces constructive and destructive interference, which is referred to as an interferogram. The beam now enters the sample compartment, where the

sample absorbs specific frequencies of energy that are unique to the sample as determined by the interferogram. The detector then measures the special interferogram signal as energy versus time for all frequencies at the same time. Meanwhile, a beam is superimposed as a reference (background) for instrument operation. Finally, the desired spectrum was obtained after the interferogram used Fourier transformation computer software to automatically subtract the background spectrum from the sample spectrum[77].

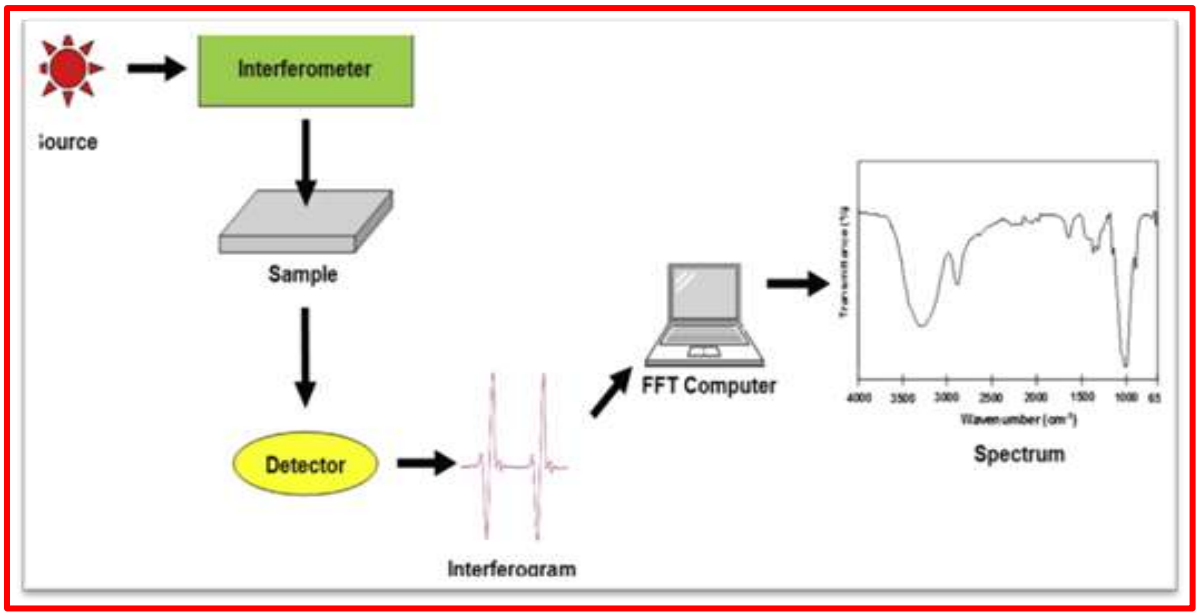

Figure (2.2). Basic component in Fourier transform infrared spectrometer[77]

2.3 The Optical Properties

The optical properties can be interpreted in light of the interaction between incident photons and samples. Furthermore, the optical properties of the sample can change or affect the incident light spectrum that passes through the sample by modifying its propagation vector or the intensity of the incident waves. The incident light spectrum of the film surface provides an overview of physical processes that can be used to investigate any sample. To discuss optical properties, optical and dielectric constants are used. Because these constants are regarded as

the most important optical parameters, their investigation is critical. The transmission and reflection measurements will be used in this study to calculate the absorption coefficient, from which the optical energy gap, electronic transition, and other parameters can be calculated [78].

2.3.1 Absorbance (A) and Transmittance (T)

a. Absorbance(A) : the absorbance is defined as the ratio of absorbed light intensity

(I_A) by material to incident light intensity (I_o). It is provided by the following relationship[79]:

$$A=I_A/I_o \quad (2.1)$$

b. Transmittance(T): Transmittance (T) is defined as the ratio of the intensity of the transmitting rays (I_T) through the material to the intensity of the incident rays (I_o) on it, and is determined by the following relationship[80]:

$$T = I_T / I_o \quad (2.2)$$

2.3.2 The electronic transitions

Electronic transitions are divided into two types [81, 82]:

1. Direct Transition

This transition occurs in semiconductors when the bottom of (C.B.) is exactly over the top of (V.B.), indicating that they have the same wave vector value, i.e. (K = 0). In this state, absorption appears when ($h\upsilon = E_g^{opt}$.) in this transition type required the Law's conservation of energy and momentum. There are two kinds of direct transitions[81, 82].

a. Direct allowed transition:

This transition occurs between the top and bottom points in the (V.B.) (C.B.).

b. Direct forbidden transitions:

This transition takes place between the near top points of (V.B.) and the bottom points of (C.B.). The absorption coefficient for this type of transition is given by[81, 82]:

$$\alpha h\upsilon = B(h\upsilon - E_g^{opt})^r \quad (2.3)$$

where E_g^{opt} is the energy difference between direct transition.

B: constant that varied depending on the material.

υ: incident photon frequency.

r: exponential constant whose value varied depending on the type of transition.

r = 1/2 for the allowed direct transition.

r = 3/2 for the forbidden direct transition.

2. Indirect Transitions

In these transitions, the bottom of (C.B.) is not over the top of (V.B.), the electron transits from (V.B.) to (C.B.) not perpendicularly, and the value of the electron's wave vector is not equal before and after the transition of the electron. ($\Delta K \neq 0$), For the conservation of energy and momentum law, this type of transition occurs with the assistance of a particle known as a "phonon." Indirect transitions are classified into two types[81, 82]:

a. Allowed indirect transitions:

These transitions occurred between the top of (V.B.) and the bottom of (C.B.), both

of which are located in a different region of the graph (K-space).

b. Forbidden indirect transitions:

These transitions occurred between near points at the top of (V.B.) and near points at the bottom of (C.B.), and the absorption coefficient for a phonon absorption transition is given by:

$$\alpha h\upsilon = B(h\upsilon - E_g^{opt} \pm E_{ph})^r \qquad (2.4)$$

where E_g denotes the energy gap for indirect transitions and E_{ph} denotes the phonon energy, which is (+) when phonon absorption and (-) when phonon emission, (r = 2) for the allowed indirect transition and (r = 3) for the forbidden indirect transition. Figure (2.3) shows Types of electronic transfers[83]

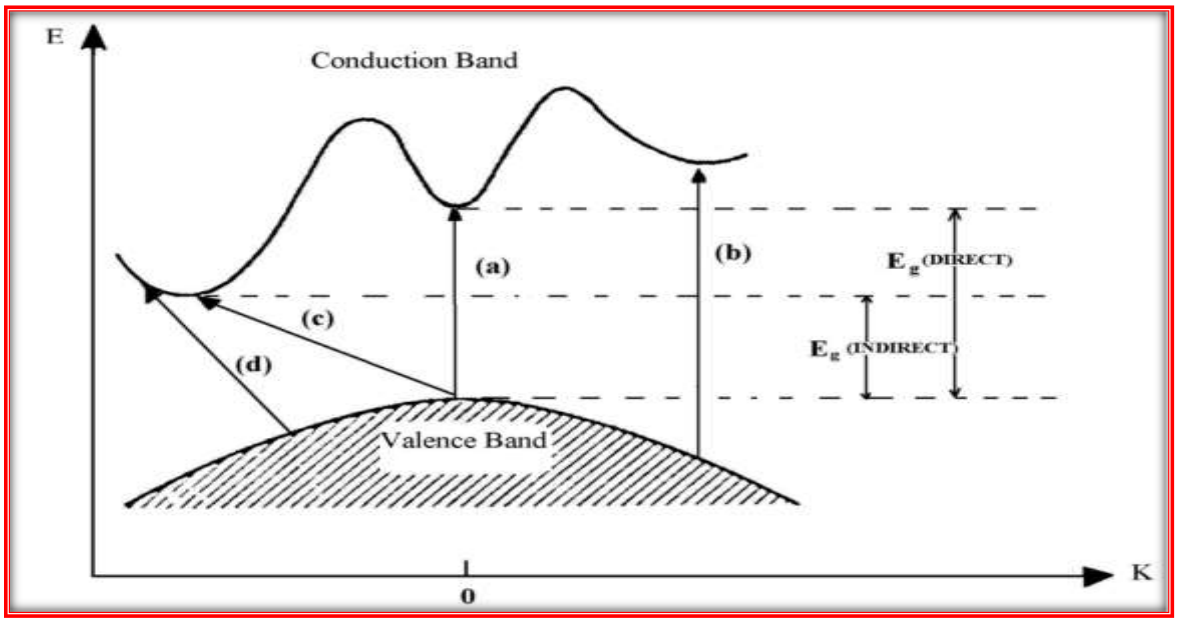

Figure (2.3). Types of electronic transfers,(a)Allowed direct, (b)Forbidden direct, (c) Allowed indirect, (d) Forbidden indirect [83]

2.3.3 Optical Constants

1. Optical absorption coefficient (α)

It is the reduction in the radiation energy incident on the material, and it is determined by the energy of the incident rays as well as the nature of the material that falls on it. The absorption coefficient is affected by the energy of the photon "hv" as well as the properties of a semiconductor, such as the type of electronic transitions and the energy gaps. The absorption coefficient is small in high wavelength and low energy, implying that the possibility of electron transition is low because the incident photon's energy is insufficient to move the electron from the valence band to the conduction band "hv> E_g. Absorption is greater at higher energies, implying that electron transitions are more likely. As a result, the incident photon's energy is sufficient to move the electron from the valence band to the conduction band, and the incident photon's energy exceeds the forbidden energy gap. The light absorption law was used to calculate the absorption coefficient[84, 85]:

$$I = I_o e^{-\alpha t} \quad (2.5)$$

Where (I_o) and (I) are the incident ray's intensities before and after passing through the material, respectively, (α) is an absorption coefficient, and (t) is the thickness of the film. It can be get after reworking the equation (2.5) above

$$\alpha = 2.303 \log (I_o/I) \quad (2.6)$$

$$\alpha = 2.303\ A/t \quad (2.7)$$

1. Extinction coefficient (k)

The extinction coefficient represents the amount of energy lost due to scattering or absorption by molecules and particles in the material. The extinction coefficient (k) is related to the interaction of incident light with material and is

associated with the absorbing power of the material, as shown by the equation[86, 87]

$$k = \alpha\lambda/4\pi \quad (2.9)$$

Where λ is the wavelength of incident light.

2. Refractive index (n)

It is the ratio of the speed of light in a vacuum to the speed of light in a medium. This index indicates the extent to which electromagnetic waves affect matter. The refraction index has two components: real and imaginary. The following equation can be used to express it[88].

$$n = c / v \quad (2.10)$$

where (n) is the refraction index, (C) is the vacuum light speed, and (v) is the matter light speed. Refractive index can be expressed by the following equation[89].

$$n = [4R/(R-1)^2 - k^2]^{1/2} + (R+1)/(R-1) \quad (2.11)$$

Reflectance (R) is also defined as the ratio of the incident ray to the reflected ray relation at the boundary line between two mediums. The following equation depicts the relationship between reflectivity and refractive index[88].

$$R = (n-1)^2 + k^2 / (n+1)^2 + k^2 \quad (2.12)$$

where (k) is the extinction coefficient. Reflectance is calculated from absorptance and transmittance by using eq [90]:

$$(R)=1-(A+T) \quad (2.13)$$

When R is reflectance, A is absorbance and T is transmittance.

4. Dielectric constant ($\mathcal{E}$)

The dielectric constant, which represents the responsiveness of electrons in the matter to the incident electromagnetic field, is frequency-dependent. Its real part 1, which represents the polarization term, and imaginary part 2 can be calculated using equation [91]:

$$\mathcal{E}_1 = n^2 - k^2 \quad (2.14)$$

$$\mathcal{E}_2 = 2nk \quad (2.15)$$

2.3.4 Optical conductivity

The optical conductivity (σ_{op}) is the electric conductivity that causes charge carriers to move due to the alternating electric field of incident electromagnetic waves, as defined by the equation below[92].

$$\sigma_{op}=\alpha nc / 4\pi \quad (2.16)$$

Where (σ_{op}) the optical conductivity, (α) is the absorption coefficient, (n) the refractive index, (c) the velocity of light.

2.4 Electrical Properties

Polymer dielectric properties have grown in importance as they provide insight into the movement of molecular chains and their applications in electrical and electronic engineering. Polymers are non-conductive because they have a very low concentration of free charge carriers. When working with sensitive electronic devices, polymers cannot provide electrostatic discharge protection. Because of this disadvantage, electrically conductive polymers, such as inherently conductive polyanilines or polymers filled with conductive particles, have been developed. The polymer becomes conductive above a critical filler concentration[93].

2.4.1 A.C electrical conductivity

When the electron distributions around constituent atoms or molecules are polarized by an external electric field, dielectric materials can be used to store electrical energy in the form of charge separation. When the electron distributions around constituent atoms or molecules are polarized by an external electric field, the complex permittivity (ε*) of a material can be expressed as energy in the form of charge separation. A material's complex permittivity (ε*) can be expressed as [94]:

$$\mathcal{E}^* = \mathcal{E}_a - j\,\mathcal{E}_b \qquad (2.17)$$

where $\mathcal{E}_a$ and $\mathcal{E}_b$ are value real and the imaginary parts of complex permittivity and Permittivity and j imaginary number equal $\sqrt{-1}$. The real part of the permittivity is given by [95]:

$$\mathcal{E}_a = \mathcal{E}_o\,\mathcal{E}' \qquad (2.18)$$

The magnitudes of $\mathcal{E}_a$ and $\mathcal{E}_b$ are affected by the angular frequency (ω) of the applied electric field. The magnitude of $\mathcal{E}_a$ (or the dielectric constant $\mathcal{E}'$) indicates a material's ability to store energy from an applied electric field. The equation gives the capacitance (C) of a capacitor made of two parallel plates[95]:

$$C = \mathcal{E}'\,\mathcal{E}_o\,A/x \qquad (2.19)$$

Where $\mathcal{E}'$ is the constant of dielectric, x is the sample thickness and $\mathcal{E}_o$ is Permittivity in vacuum. Dielectric constant is given by the relation[96]:

$$\mathcal{E}' = C_P / C_o \qquad (2.20)$$

Where C_p denotes parallel capacitance and Co denotes vacuum capacitance, which can be calculated by using[96]:

$$C_o = \mathcal{E}_o\,a / t \qquad (2.21)$$

Where ε is vacuum permittivity, a: is the area of the capacitance plate, t: is the distance between two plates. Dielectric loss Ɛ″ can be calculated by the relation[97]:

$$\mathcal{E}'' = \mathcal{E}' D \qquad (2.22)$$

Where D is the dispersion factor, The a.c. conductivity (σa.c) was calculated according to the following relation[98]:

$$\sigma A.C = \omega \mathcal{E}_o \mathcal{E}'' \qquad (2.23)$$

where ω is an angular frequency ($\omega = 2\pi f$).

2.5 Antibacterial Application

The ability to integrate nanotechnology with biotechnology ensures the greatest impact in biology and biomedicine because the convergence of these two fields gives rise to a combinatorial field of nanobiotechnology. Nanomaterials have sparked interest due to their distinct optical and electronic properties. when compared to bulk states, these novel properties of this class of materials make them extremely promising for a wide range of industrial, technological, and biomedical applications. Antibacterial materials are increasingly in demand in a variety of industries, including textiles, food, water disinfection, medicine, and food packaging. The resistance of some bacteria to antibiotics and the toxicity of some organic antimicrobial substances to the human body have increased interest in the development of inorganic antimicrobial substances [97, 98]. Metal and metal oxide compounds have gotten a lot of attention because of their broad-spectrum antibacterial properties. Metal oxides with antibacterial properties, such as TiO_2, SiO_2, and ZnO, have been deposited on transparent substrates using various coating methods. Bacterial resistance to antibacterial drugs develops through a variety of mechanisms, necessitating a new approach to developing new

bactericidal drugs. The search for new antimicrobial agents or modifications to existing ones to improve antimicrobial activity has become essential. Nanotechnology provides an excellent platform for modifying the physicochemical properties of various materials in comparison to their bulk counterparts, which can then be used for biomedical applications. Nanomedicine, an offshoot of nanotechnology, has made significant advances in disease diagnosis, monitoring, drug delivery, and control[99].

2.5.1 The antibacterial mechanisms of nanomaterial

Although the exact mechanism of nanoparticles' antibacterial effects has not been entirely clarified, various antibacterial actions have been proposed nanoparticles can continually release ions, which may be considered the mechanism of killing microbes. Owing to electrostatic attraction , ions can adhere to the cell wall and cytoplasm. membrane. The adhered ions can enhance the permeability of the cytoplasmic membrane and lead to disruption of the bacterial envelope. After the uptake of free ions into cells, respiratory enzymes can be deactivated, generating reactive oxygen species but interrupting adenosine triphosphate production. Reactive oxygen species can be a principal agent in the provocation of cell membrane disruption and deoxyribonucleic acid (DNA) modification. As sulfur and phosphorus are important components of DNA, the interaction of ions with the sulfur and phosphorus of DNA can cause problems in DNA replication, cell reproduction, or even result in the termination of the microorganisms. Moreover, ions can inhibit the synthesis of proteins by denaturing ribosomes in the cytoplasm[100].

In addition to being able to release ions, nanoparticles can themselves kill bacteria. Silver nanoparticles can accumulate in the pits that form on the cell wall after they anchor to the cell surface. The dissolution status of nanoparticles in exposure media strongly affects their antibacterial effect and mechanism. The dissolution efficiency depends on synthetic and processing factors, such as intrinsic silver nanoparticle characteristics and surrounding media[100].

2.6 Gamma ray shielding application

Metals have traditionally been used as materials for electromagnetic shielding, but they have drawbacks such as high cost, large weight, poor adhesion, corrosion in extreme environments, and poor processability. Conducting polymers differ from metals in that they not only reflect but also selectively absorb electromagnetic radiation. Because of these properties, conducting polymers are useful in radar or microwave-absorbing formulations used in military and civil applications such as stealth technology[101]. The absorption of radiation is characterized by the equation[102]:

$$N=N_0 \exp(-\mu x) \tag{2.24}$$

where N_0 is the number of particles of radiation counted during a certain time duration without any absorber, N is the number counted during the same time with a thickness x of absorber between the source of radiation and the detector, and μ is the attenuation coefficient of gamma radiation. With the increased use of active gamma-ray isotopes in industry, medicine, and agriculture, it is now necessary to investigate mass attenuation coefficients in a variety of materials of technological and biological significance. There is always a need to develop a material that can be used as a shield under the harsh conditions of nuclear radiation exposure.

Because nuclear radiation shielding necessitates a greater quantity of shielding material, the study of radiation flux propagation in shielding materials is an essential requirement for shield design[103]. Many research efforts have been made to develop more efficient shielding materials that may be capable of attenuating gamma as well as being lightweight, cost-effective, portable, and adaptable. Polymeric nanocomposites with a controlled microstructure on a nanometer to sub-micron scale have a high potential for producing highly functional materials with unusual physical properties. Polymer composites are suitable candidates for solving traditional shielding problems [79]. To create effective radiation shields, nanomaterials dispersed in a polymer matrix can be used. The attenuation is achieved through the combination of nanoparticles and polymers. Polymer-based composites are particularly appealing as radiation-shielding materials for a variety of reasons. They are lighter than their metal counterparts and can be processed to achieve effective shielding for specific industrial radiations. Polymer nanocomposites combine nanoparticles' excellent functional properties[104].

Chapter Three

Experimental Part

3.1 Introduction

This chapter covers sample preparation, processing, and measurement stages such as optical microscopy, FTIR, SEM, optical measurements, A.C electrical property measurements, and antibacterial activity measurements.

3.2 The Materials Used in this Work

3.2.1 Matrix Material

3.2.1.1 Poly (methyl methacrylate) PMMA

Poly (methyl methacrylate), also known as acrylic, is a transparent thermoplastic as shown in figure (3.1). It has a melting point of about (220-240) C^{o} and a density (1.18) g/cm^{3}.

Figure (3.1). Poly (methyl methacrylate) Polymer

3.2.1.2 polyethylene Glycol (PEG)

Polyethylene glycol (PEG) is used in a variety of applications. It has a melting point of about (54–58 C^{o}) and its density is about (1.1–1.2) g/cm^{3} . Figure (3.2) shows polyethylene glycol.

Figure (3.2). Polyethylene glycol Polymer

3.2.2 Additive Material

One type of additive nanomaterial is used in this work is:

Silicon nitride (Si_3N_4)

Silicon nitride is used as a powder additive for polymer matrix, as shown in Figure (3.3). The silicon nitride (Si_3N_4, 15-30 nm, purity 99.9 %) was obtained from Nanoshel, Wilmington, DE- 19808 USA. It has a melting point of about (1900 Co) and its density is about (3.17–3.20) g/cm3. It is used in a variety of applications.

Figure (3.3). Silicon nitride

3.3 Preparation of (PMMA-PEG-Si_3N_4) Nanocomposites

The nanocomposite (PMMA-PEG/Si_3N_4) were prepared by (1 gm) of the polymeric material (0.85 gm of polymethyl methacrylate and 0.15 gm of polyethylene glycol) was dissolved in (30) ml of chloroform alcohol, and the solution was thoroughly mixed for one hour with a magnetic stirrer. The Si_3N_4 nanoparticles are added to the (PMMA-PEG) with varying concentrations (1.6,3.2,4.8, and 6.4) wt%. The casting method is used to prepare samples of (PMMA-PEG/Si_3N_4) nanocomposites in a template (a Petri dish with a diameter of 10 cm) and allow them to dry . Figure (3.1) shows the outline for the practical part

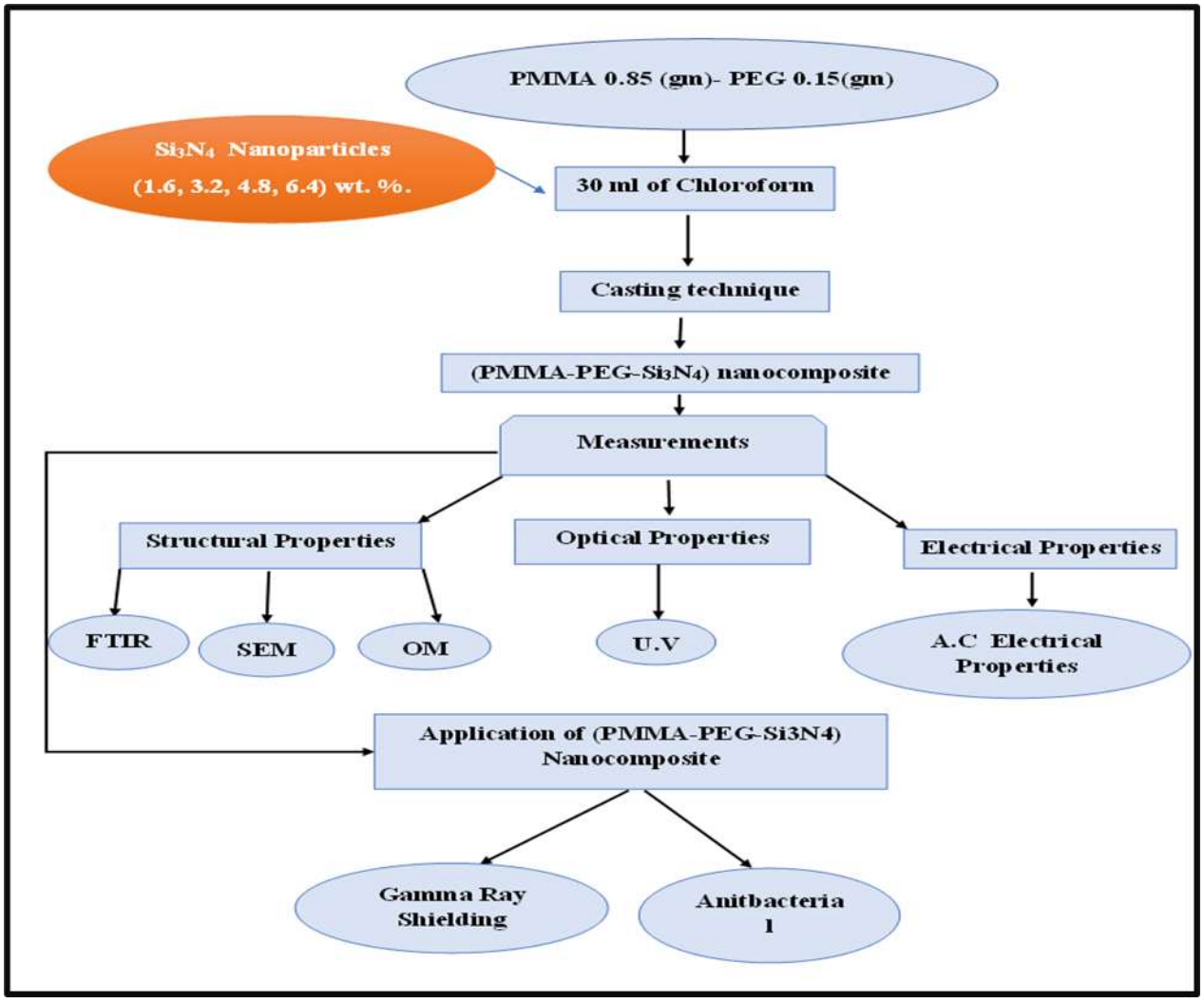

Figure (3.4) The outline represents the practical part

3.4 Measurements of Structural Properties for Nanocomposites

3.4.1 Optical Microscope (OM)

Samples of nanocomposites (PMMA-PEG/Si_3N_4) were examined by using the optical microscope named Olympus (top view) type (Nikon 73346) under magnification (10x). This measurement was made at the University of Babylon/College of Education for pure sciences.

Figure (3.5). Optical Microscope used in the work

3.4.2 FTIR spectrometer

FTIR spectra of (PMMA-PEG/Si_3N_4) were recorded by FTIR (Brucker Company), German origin, type vertex-70) Fourier transform infrared spectrometer in the wavelength range (500-4000) cm-1, in the College of Education for Pure Sciences, University of Babylon

Figure (3.6). Fourier transform infrared spectroscopy device used in the work

3.4.3 Scanning Electron Microscope (SEM)

The surface morphology of (PMMA-PEG/Si_3N_4) nanocomposites was tested using a scanning electron microscope, at the Shahrud University of Technology, Iran, It is characterized by magnifying the image with a high accuracy of about 100,000 times, as a beam of electrons is directed to the surface and gives black-and-white images of the sample surface because it does not depend on light waves but on electronic emission.

3.5 Measurements of Optical Properties for Nanocomposites

The optical properties of (PMMA-PEG/Si_3N_4) nanocomposite samples were measured using a double-beam spectrophotometer (Shimadzu, UV-18000A) at wavelengths (240-840) nm. This measurement was implemented in the University of Babylon College of / Education for Pure Sciences as shown in Figure (3.7).

Figure (3.7). UV–Visible Spectrophotometer (Shimadzu-1800).

3.6 Measurements of A.C Electrical Conductivity Properties for (PMMA-PEG-Si3N4) Nanocomposites

The A.C electrical conductivity was measured with a frequency ranging (100Hz- 5 MHz) LCR meter (HIOKI 3532-50 LCR Hi TESTER (Japan)) located in the University of Babylon/College of Education for Pure Sciences/Department of Physics. Capacitance (CP) and dispersion factor (D) were recorded for all samples. The dielectric constant, dielectric losses, and conductivity were measured at room temperature. Figure (3.8) shows a diagram for the A.C electrical measurement system

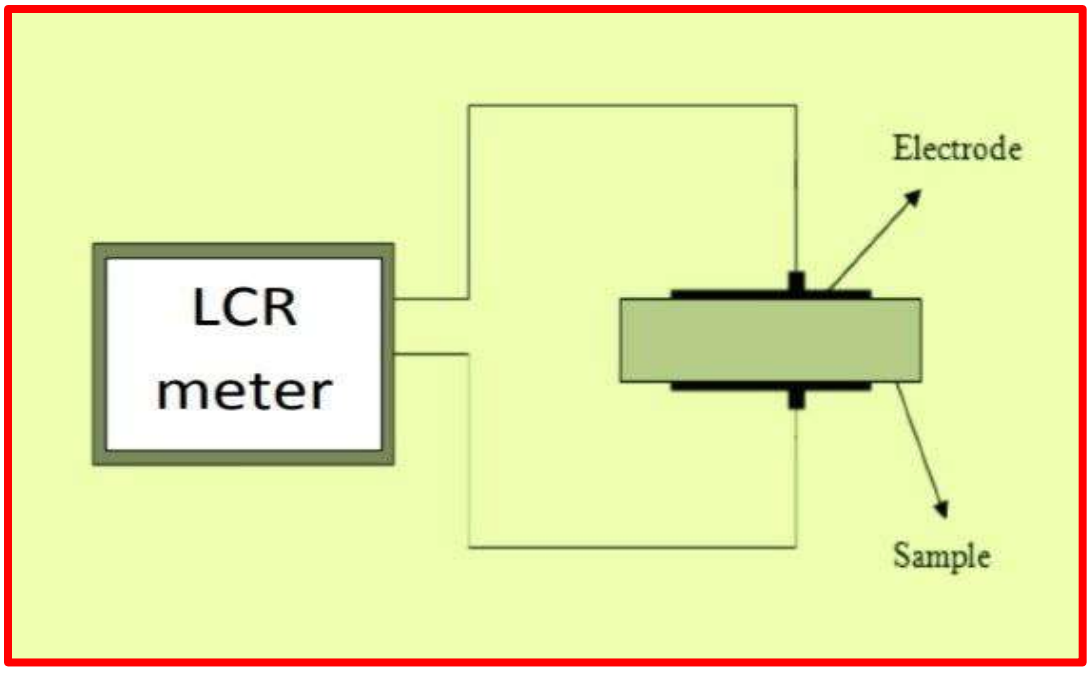

Figure (3.8). Diagram for system of A.C electrical measurement system

3.7 Measurements of Anti-bacterial Activity for Nanocomposites

The antibacterial activity of (PMMA-PEG/Si_3N_4) nanocomposites samples was tested by diffusion method. Antibacterial activities were carried out using Gram-positive (Staphylococcus aureus) and Gram-negative (Escherichia coli) organisms. Bacteria (Staphylococcus aureus and Escherichia coli) were cultured in

Muller-Hinton Medium. Discs (PMMA-PEG/Si_3N_4) were placed on media and incubated at (37°C) for 24 hours. The diameter of the damping zone was measured.

3.8 Gamma Ray Shielding Application Measurements of Nanocomposites

Gamma-ray shielding measurements of (PMMA-PEG/Si_3N_4) nanocomposites have been performed to examine the attenuation properties of gamma rays for the specimens with various concentrations of (Si_3N_4) nanoparticles. Test specimens with varying concentrations were ordered in front of the parallel beam emanating from the gamma-ray exporter (Cs-137). The gamma-ray exporter is situated at a distance of (3) cm from the detector. The emitted gamma ray influxes through the specimens are determined by the Geiger counter which is used for an estimate the linear attenuation coefficient. This measurement was implemented in the University of Babylon College of / Education for Pure Sciences as shown in figure (3.9)

Figure (3.9). Gamma-ray shielding

Chapter Four

Results and Discussion

4.1 Introduction

This chapter includes the results and discussion of the structural, optical, A.C electrical properties and applications for antibacterial activity and gamma sheliding of (PMMA-PEG/Si_3N_4) nanocomposites.

4 .2 Structural Properties of (PMMA-PEG/Si_3N_4) nanocomposites

4.2.1 Optical Microscope (OM) and Scanning Electronic Microscope (SEM) of (PMMA-PEG-Si_3N_4)

Figure (4.1) shows the image of the optical microscope for (PMMA-PEG /Si_3N_4) nanocomposites at magnification power (X10) for all the samples. The figure shows the nanoparticle Si_3N_4 arrangements in (PMMA/PEG-Si_3N_4) nanocomposite, where at lower concentrations, the Si_3N_4 nanoparticles form a clusters. When the concentrations of Si_3N_4 nanoparticles in the (PMMA-PEG) blend increase, the nanoparticles form a network of paths inside the (PMMA-PEG) blend which charge carriers can pass, leading to a change in the material properties. This behavior agrees with the researchers' results [105, 106]. SEM analysis was used to investigate the structure and distribution of Si_3N_4 nanoparticles in a polymer blend (PMMA-PEG). Figure (4.2) shows the SEM images of the (PMMA-PEG-Si_3N_4) nanocomposite in various concentrations of Si_3N_4 NPS. SEM images of pure (PMMA-PEG) blend show that the surface is relatively rough. The nanocomposite contains numerous Si_3N_4 particles that are finely dispersed without aggregates and are widely distributed across the surface. Nanoparticles are distributed in spherical form, similar to grain, and are randomly distributed on the surface. This behavior agrees with the researchers' results [107, 108] .

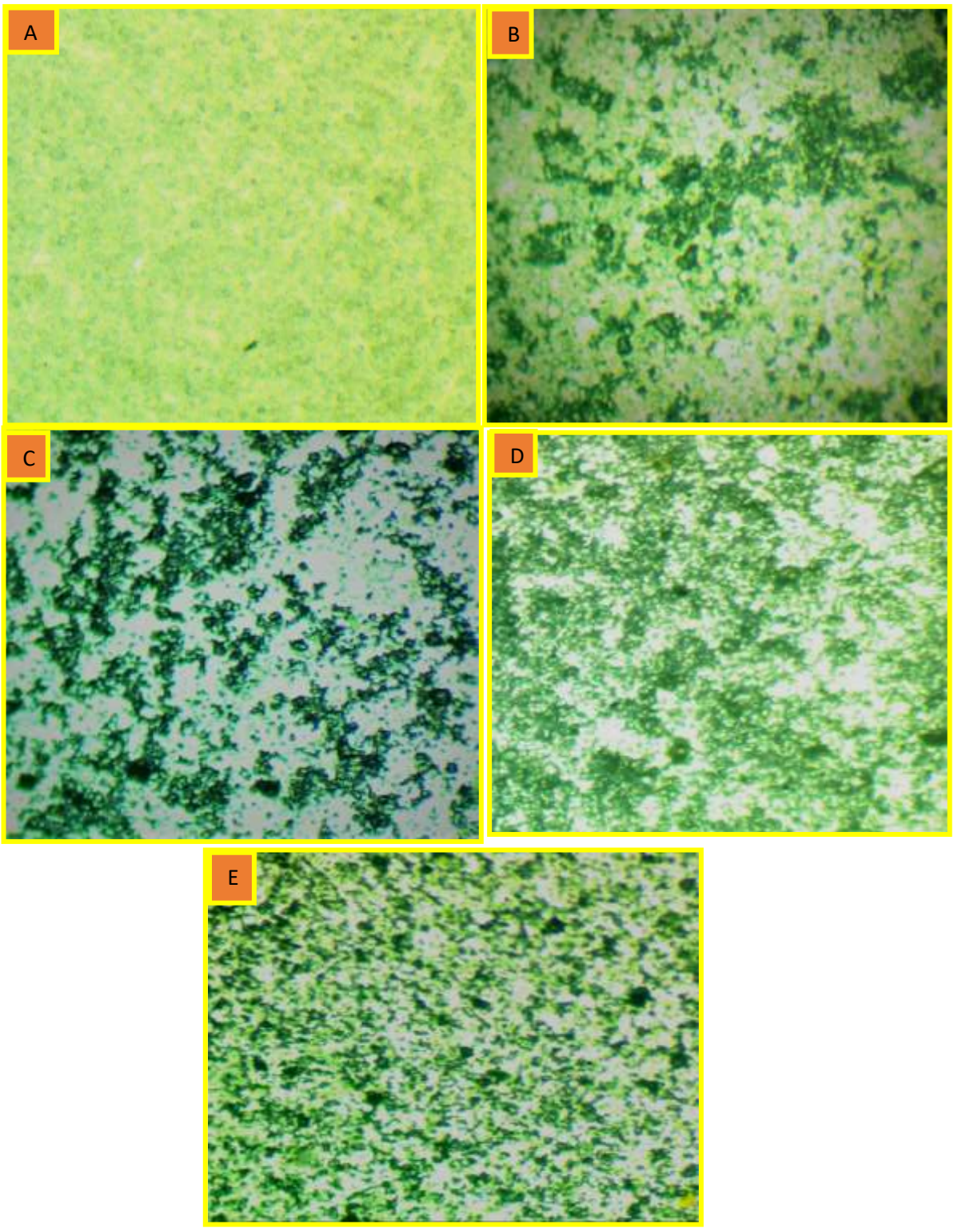

Figure (4.1). Microscope images (X10) for (PMMA-PEG/Si3N4) nanocomposites:(A) for blend, (B) 1.6 wt.% ,(C) 3.2 wt.%, (D) 4.8 wt.% and (E) 6.4 wt.%

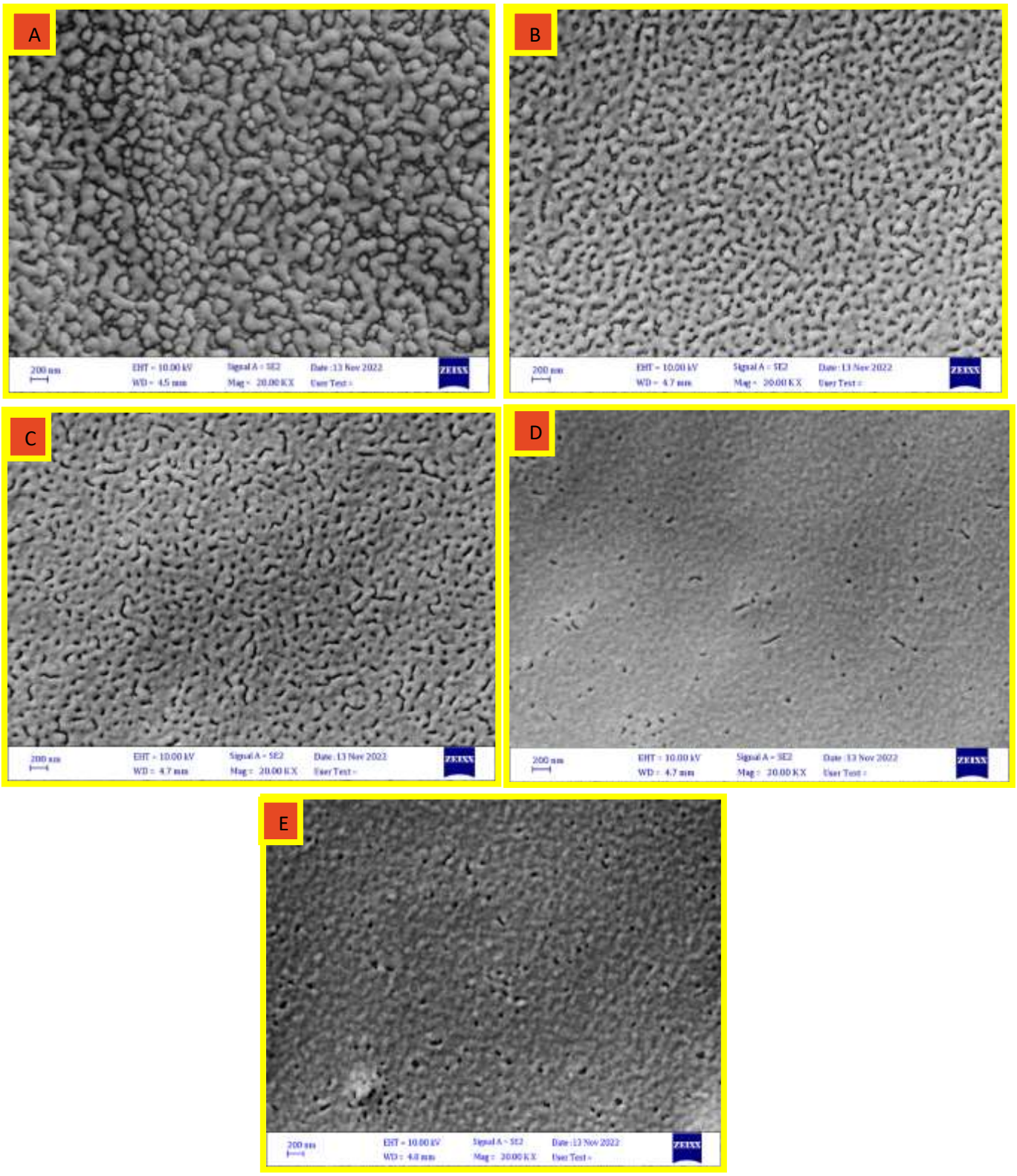

Figure. (4.2). SEM images for (PMMA-PEG/Si_3N_4) nanocomposites A. for blend, B 1.6 Wt.%, C. 3.2 Wt.%, D. 4.8 Wt.%, E. 6.4 Wt.%

4.2.2 Fourier Transform Infrared Radiation (FTIR) of (PMMA-PEG/Si_3N_4) Nanocomposites

FTIR analysis of the (PMMA-PEG/Si_3N_4) nanocomposite at wavenumber ranges (1000-4000) cm^{-1} are shown in figure (4.3). The peak at around (2950.01) cm^{-1}, can be customized for an asymmetric stretching mode of the CH_2 group associated with PMMA. The distinctive peak at around (1723.96) cm^{-1} resulting from carbonyl stretch vibration C=O essentially represents the PMMA and PEG interference. The peak at wave number (1435.15) cm^{-1} is due to C-O groups in the polymer matrix. The bands at (1238.52) are associated with the C-C-O expansion in the ester group. The distinctive bands at (1143.52- 985.74) are due to the -CH_2. In addition, all the FTIR curves of the Si3N4 complexes present clear characteristic absorption peaks near (952 and 447) cm^{-1}, owing to the incorporation of Si_3N_4 nanoparticle. FTIR studies show no interactions between the polymer matrix (PMMA-PEG) and Si_3N_4 nanoparticles. When the concentrations of Si_3N_4 NPs content increase, "the transmission" decreases due to the increased density of nanocomposites[95,109,110].

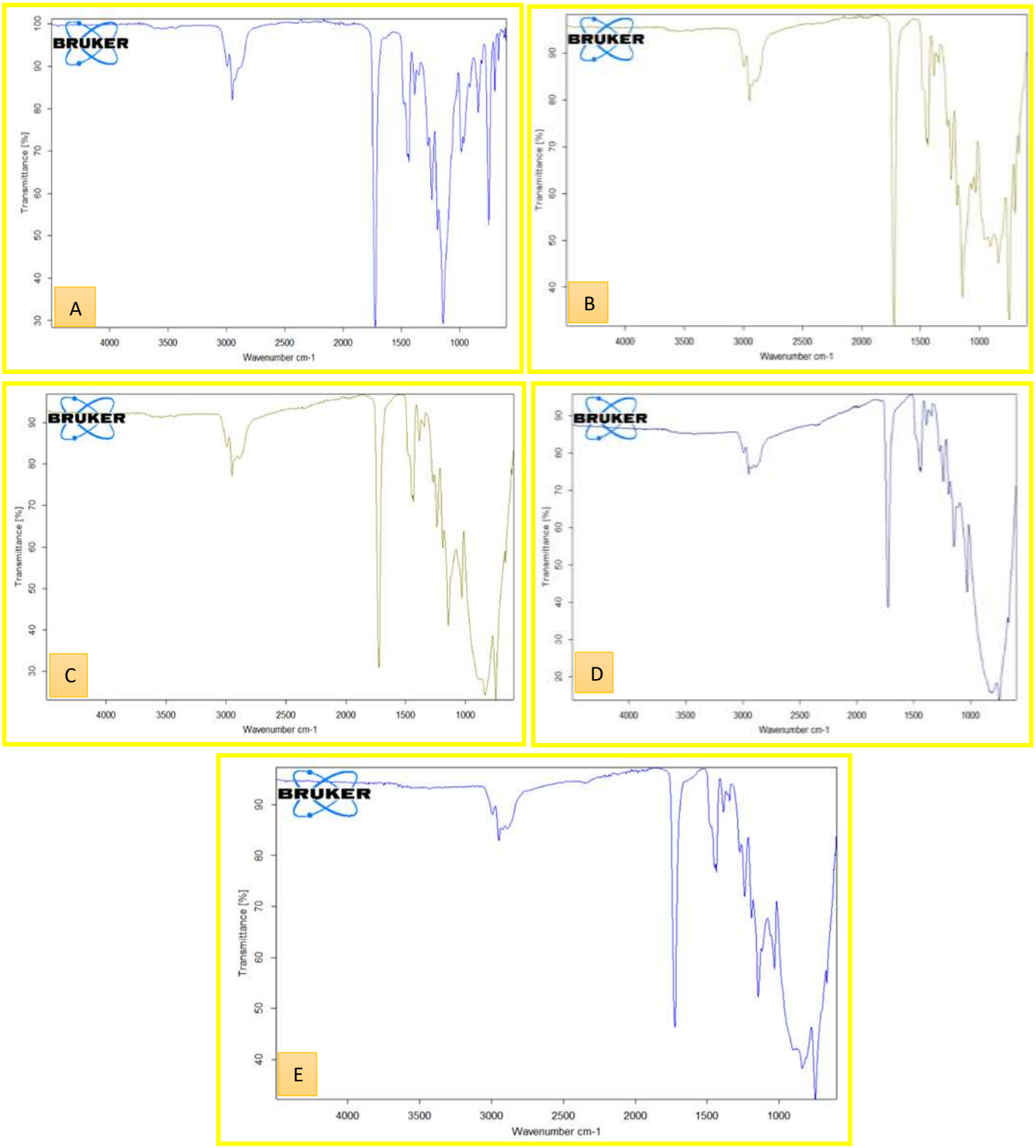

Figure (4.3). FT-IR spectra (PMMA-PEG/Si_3N_4) nanocomposites: (A) for blend, (B) 1.6 wt.%, (C) 3.2 wt.%, (D) 4.8 wt.% and (E) 6.4 wt.%

4.3 The Results of Optical Properties

4.3.1 Absorbance and transmittance of (PMMA-PEG/Si_3N_4) nanocomposites

Figures (4.4) and (4.5) show the absorbance and transmittance spectra of (PMMA-PEG/Si_3N_4) nanocomposites as a function of incident light wavelength. It is obvious that the addition of silicon nitride (Si_3N_4) to (PMMA-PEG) blend lead to increase the intensity of the absorbance in the short wavelength region and shifts the position of the absorption edge towards red wavelengths for all Si_3N_4 concentrations. The fact that Si_3N_4 atoms absorb incident light can explain the increase in absorbance with an increasing Si_3N_4 NPS content[103,104]. Furthermore, a slight shift in the absorption edge toward the high-wavelength region indicates that the optical band gap has shrunk. In addition to the absence of an absorption band in the visible region, this means the samples are transparent, this behavior agrees with the researchers' results[111,112]. The transmittance decreases as the concentration of Si_3N_4 NPS increases, this is due to the silicon nitride Si_3N_4 NPS that contains electrons in its outer orbits, which absorb the electromagnetic energy of the incident light, resulting in electron transition to higher energy levels, because the electrons that moved to higher levels occupied vacant positions of energy bands, part of the incident light is absorbed by the substance and does not penetrate through it[113]. On the other hand, (PMMA-PEG) blend has high transmittance because there are no free electrons (i.e .electrons are linked to atoms by covalent bonds), this behavior agrees with the researcher results [113].

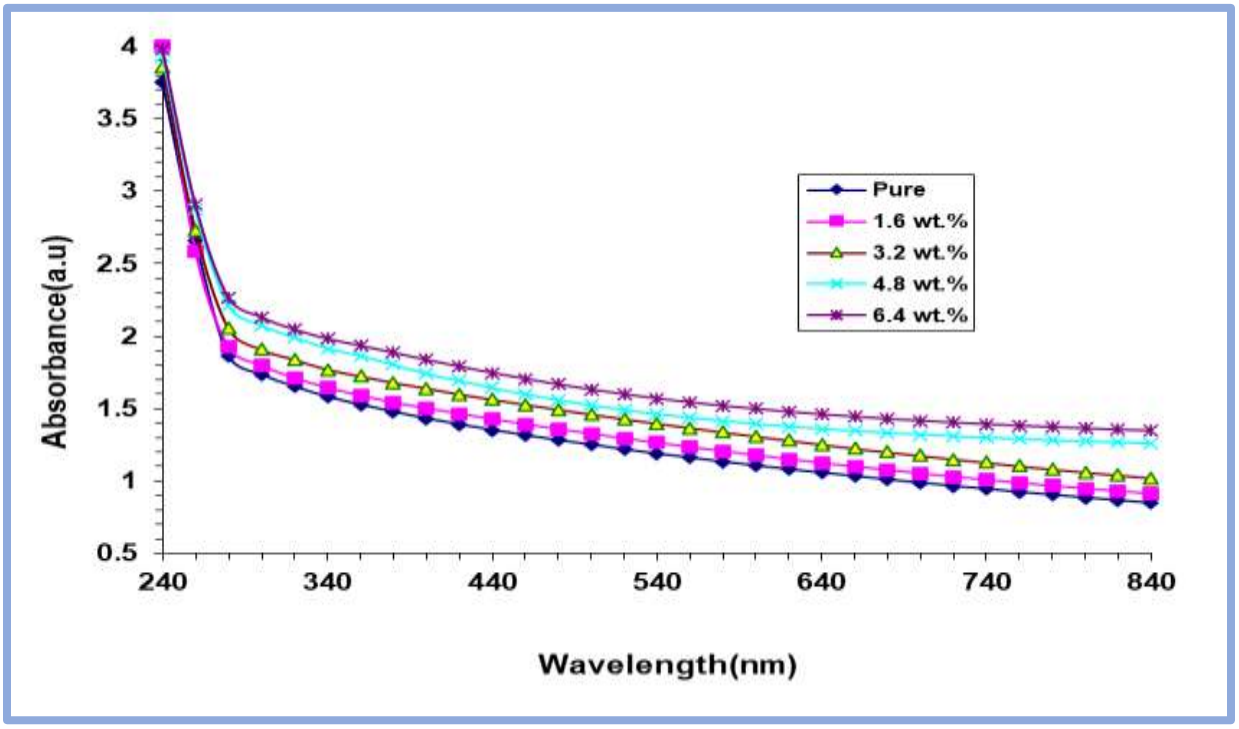

Figure (4.4). Variation of absorbance for (PMM-APEG /Si_3N_4) nanocomposites with Wavelength

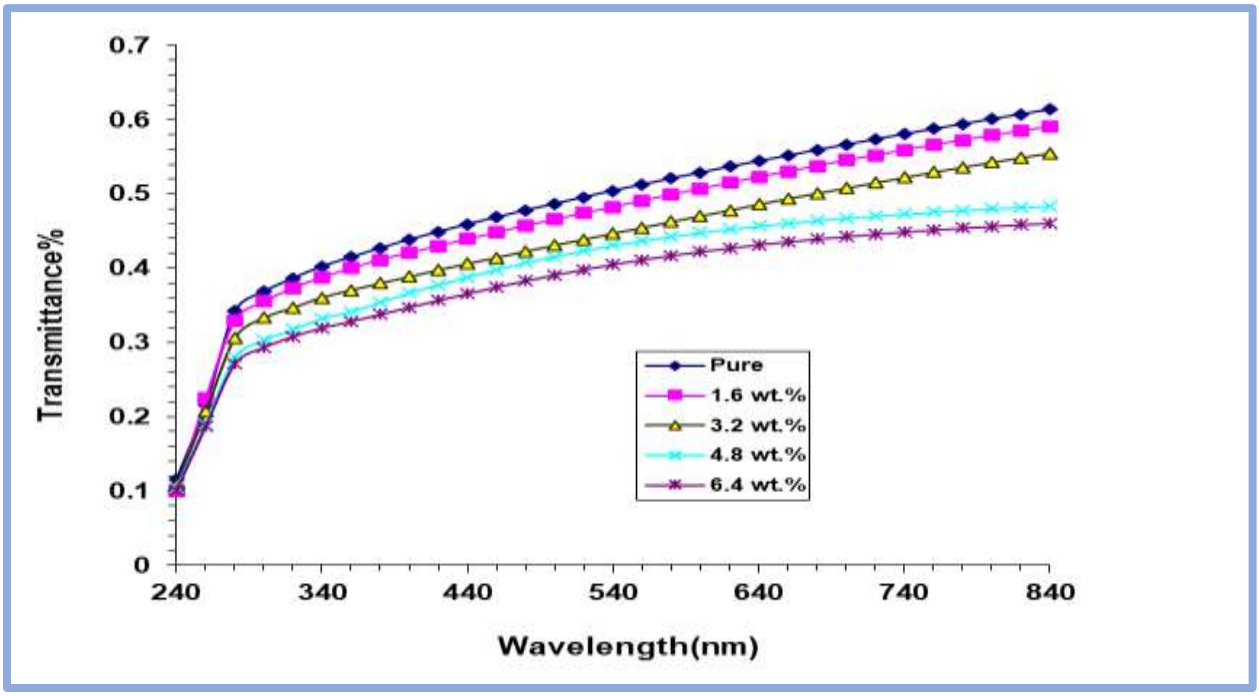

Figure (4.5). Variation of transmittance for (PMMA-PEG/Si_3N_4) nanocomposites with wavelength

4.3.2 Absorption coefficient (α) of (PMMA-PEG/Si_3N_4) nanocomposites

The variation of the absorption coefficient for (PMMA-PEG/Si_3N_4) nanocomposites with photon energy is shown in Figure (4.6). It can be seen that the absorption coefficient is the smallest at low energy, indicating that the possibility of an electron transition is low because the energy of the incident photon is insufficient to move the electron from the valence band to the conduction band ($h\upsilon<Eg$). Absorption is greater at higher energies, implying that electrical transitions are more likely. As a result, the incident photon's energy is sufficient to move the electron from the valence band to the conduction band, and the incident photon's energy exceeds the forbidden energy gap. This demonstrates that when the absorption coefficient is high ($\alpha>10^4$ cm^{-1}), it is aide in determining the nature of the electron transition. However, when the absorption coefficient is low ($\alpha<10^4$) cm^{-1} ,this mean the indirect transition of electrons is expected to occur, and the electronic momentum is maintained with the help of the phonon [114,115]. As a result, the coefficient of absorption for the (PMMA-PEG/Si_3N_4) nanocomposites is less than 10^4 cm^{-1} at all concentration. The absorption coefficient of nanocomposites increases with increasing concentrations of (Si_3N_4) nanoparticles, which is attributed to an increase in the number of charge carriers, resulting in an increase in absorbance and the absorption coefficient for the nanocomposite. This behavior agrees with the researchers' results [114,115].

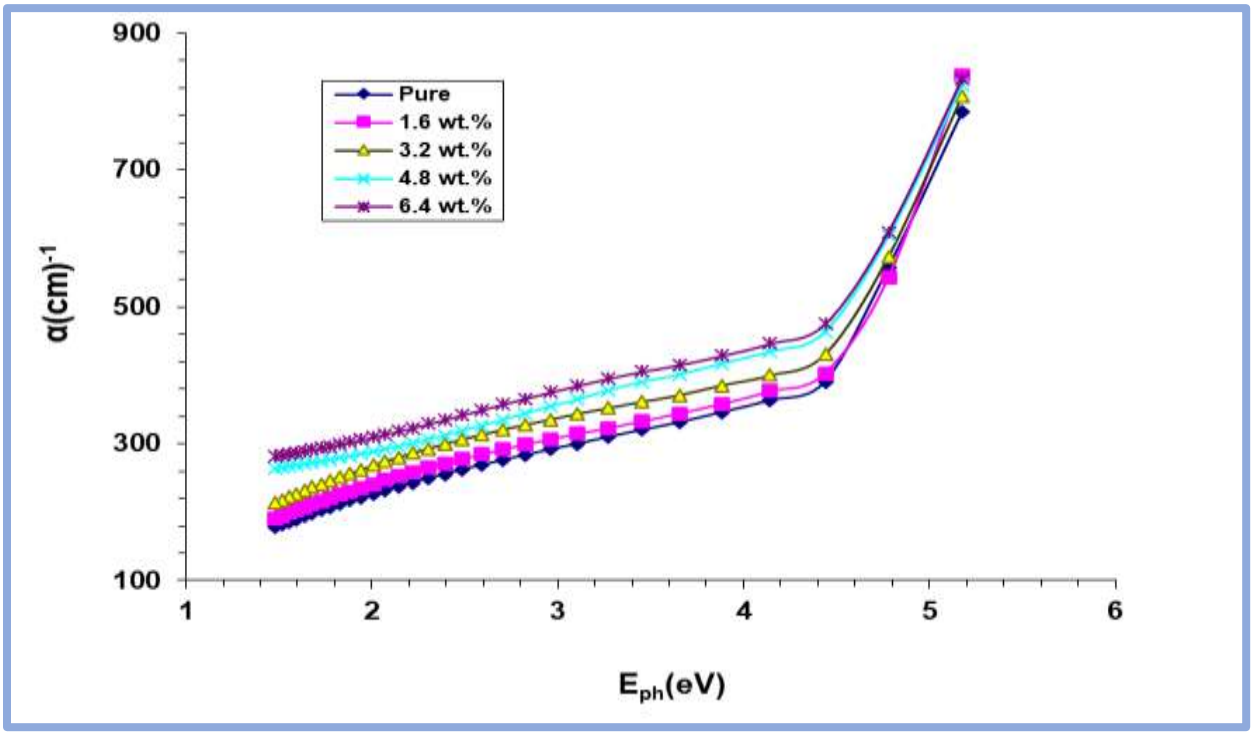

Figure (4.6). Variation of absorbance coefficient (α) for (PMMA-PEG/Si_3N_4) nanocomposites with photon energy

4.3.3 Extinction coefficient (k) of (PMMA-PEG/Si_3N_4) nanocomposites

The extinction coefficient of (PMMA-PEG/Si_3N_4) nanocomposites as a function of photon wavelength is depicted in Figure (4.7). The extinction coefficient represents When an electromagnetic wave propagates through a material, the amount of absorption loss, which is a measure of the fraction of light lost due to scattering and absorption per unit distance of a penetration medium. The decrease in the extinction coefficient with increasing photon energy represents an increase in the fraction of light lost due to scattering and absorbance. Furthermore, as photon energy increases, the loss factor decreases. because the Si_3N_4 NPS absorbed the photon [116,117].The extinction coefficient of nanocomposites increases as the concentration of Si_3N_4 nanoparticles increases, this is due to increased optical

absorption and photon dispersion in the (PMMA-PEG) polymer matrix[110]. This behavior agrees with the researchers' results [116, 117].

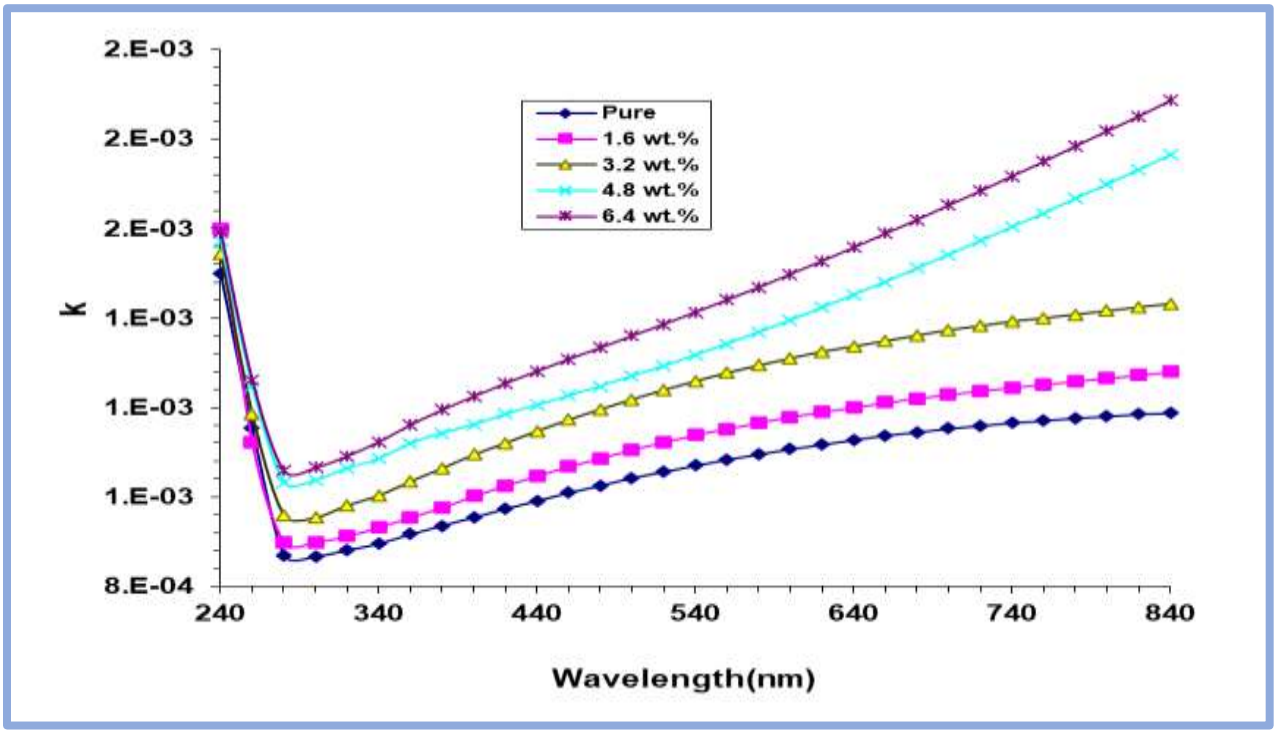

Figure (4.7). Variation of extinction coefficient for (PMMA-PEG/Si_3N_4) nanocomposites with wavelength

4.3.4 Refractive index (n) of (PMMA-PEG/Si_3N_4) nanocomposites

Figure (4.8) depicts the change in refraction index as a function of wavelength for (PMMA-PEG/Si_3N_4). The refractive index of (PMMA-PEG/Si_3N_4) nanocomposites decreases with increasing wavelength. The refractive index is primarily determined by reflectance. As a result, it can be observed that the increase in refractive index by increasing the concentration of Si_3N_4 because the reflectance increases, this behavior is attributed to an increase in density with increasing concentration[81]. The refractive index is high in the ultraviolet region

due to the low transmittance in this region, but low in the visible and near IR regions due to the high transmittance in this region, this behavior agree with[81,118].

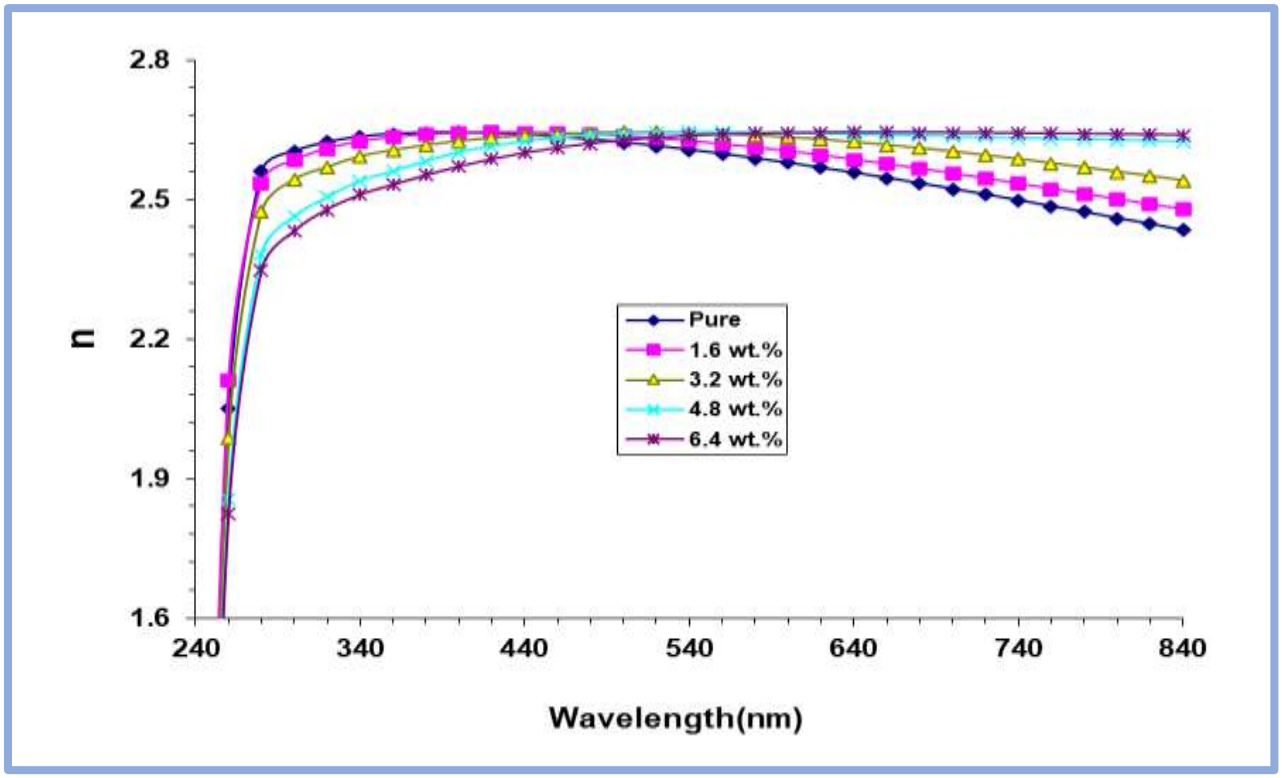

Figure (4.8). Variation of refractive index for (PMMA-PEG/Si_3N_4) nanocomposites with wavelength

4.3.5 Energy gap of (PMMA-PEG/Si_3N_4) nanocomposites

Figures (4.9) and (4.10) show the energy gap values of (PMMA-PEG/Si_3N_4) nanocomposites for allowed and forbidden indirect transitions. The allowed and forbidden indirect transition optical energy gap, when r=2, the optical energy gap of the allowed indirect transition is calculated, when r=3, the optical energy gap of the forbidden indirect transition is calculated. It can be seen that the optical energy gap values decrease as the content of (Si_3N_4) nanoparticles increases. This is attributed to the formation of site levels in the forbidden optical energy gap; in this

case, the transition is carried out in two stages, with electrons transitioning from the valence band to the local levels to the conduction band as the Si_3N_4 nanoparticle content increases[119]. This behavior is attributed to the fact that nanocomposites are heterogeneous (i.e., electronic conduction depends on added concentration), the increase of silicon nitride nanoparticles provides electronic paths in the polymer, facilitating the crossing of electrons from the valance band to the conduction band, which explains the decrease of optical energy gap with the increase of Si_3N_4 nanoparticles. This behavior agrees with the researcher's results [120].

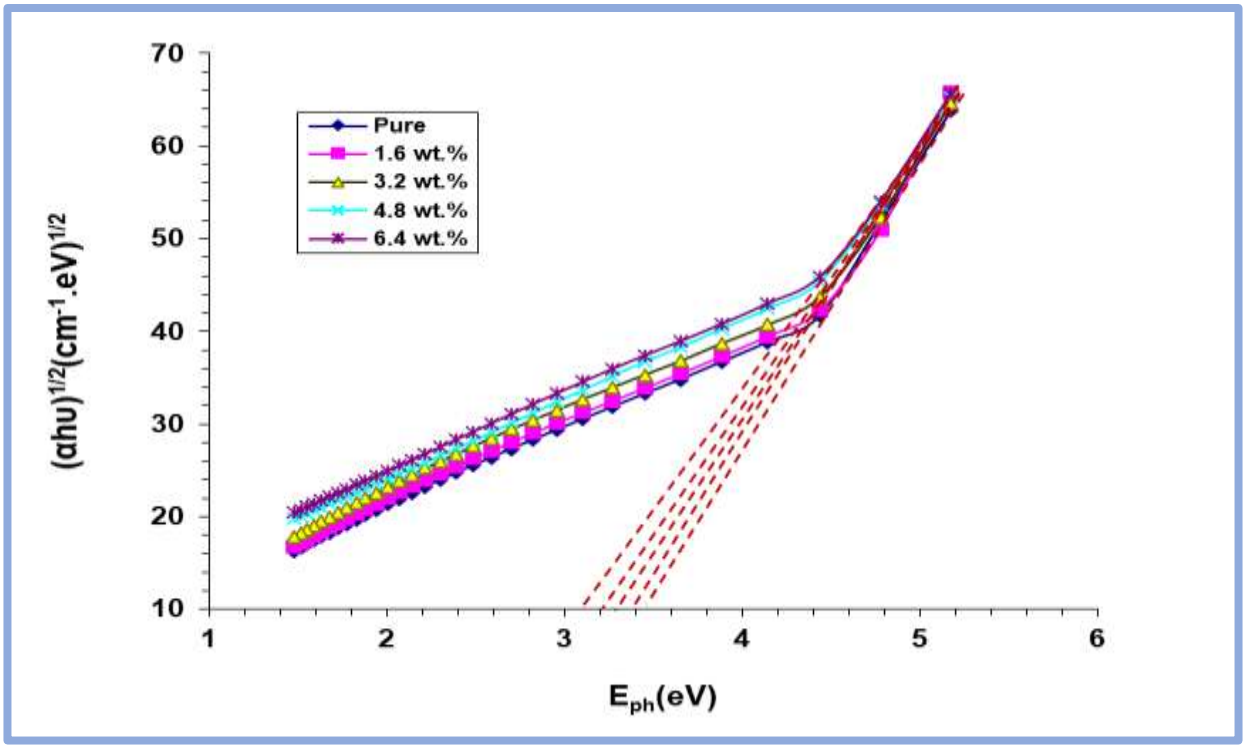

Figure (4.9). Variation of $(\alpha hv)^{1/2}$ for (PMMA-PEG/Si_3N_4) nanocomposites with E_{ph}

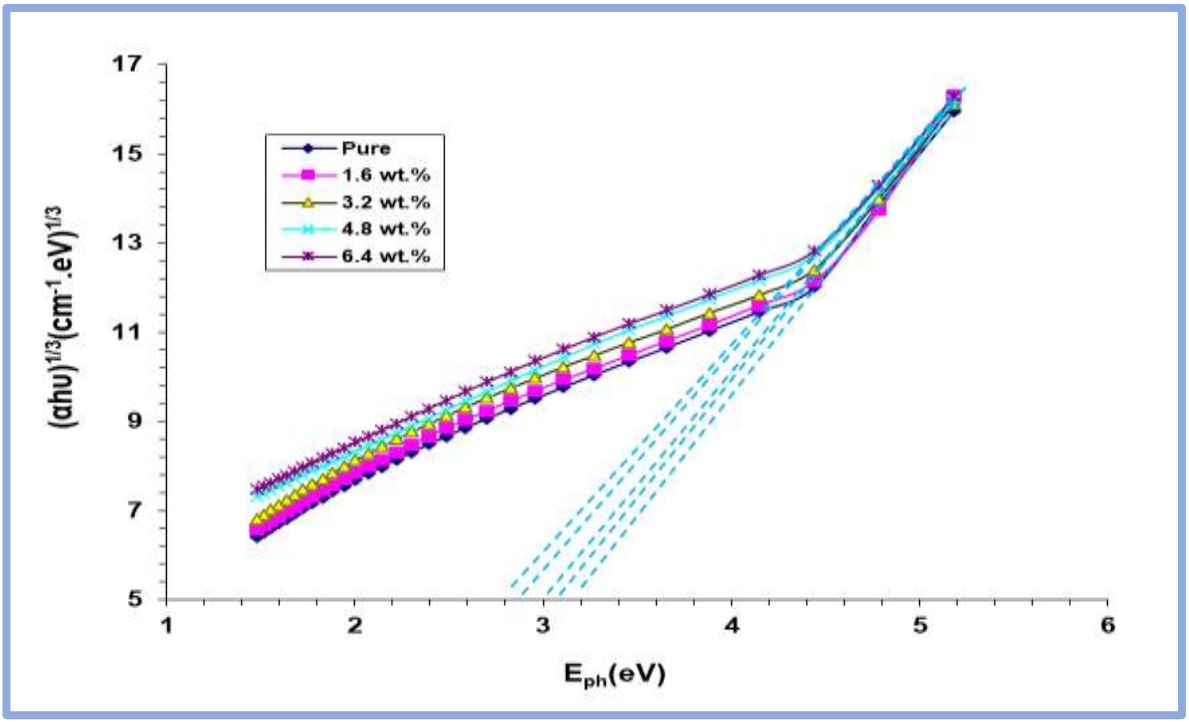

Figure (4.10). Variation of $(\alpha h\upsilon)^{1/3}$ for (PMMA-PEG/Si_3N_4) nanocomposites with E_{ph}

4.3.6 The Real and imaginary parts of dielectric constant (ε_1 and ε_2)

Figure (4.11) shows the behavior of the real part of the dielectric constant with wavelength for (PMMA-PEG/Si_3N_4) nanocomposites. Figure (4.12) depicts the effect of Si_3N_4 nanoparticles concentrations on the imaginary part of the dielectric constant. The figures show that the real and imaginary parts of the dielectric constant of the (PMMA-PEG) blend increase as the concentration of Si_3N_4 nanoparticles increases. This behavior is attributed to an increase in electrical polarization due to the contribution of Si_3N_4 nanoparticle concentration in the sample, i.e., the increase in the dielectric constant of (PMMA-PEG) blend represents a fractional increase in charges within the polymers. As shown in the figures, the real and imaginary parts of the dielectric constant of a (PMMA-PEG/Si_3N_4) nanocomposite change with wavelength. This is because the real part of the dielectric constant is affected by refractive index[121]. The imaginary part

of the dielectric constant is dependent on the extinction coefficient, particularly in the visible and near-infrared wavelength regions where the refractive index is approximately constant while the extinction coefficient increases with wavelength increase. This behavior agrees with the researcher's results [122].

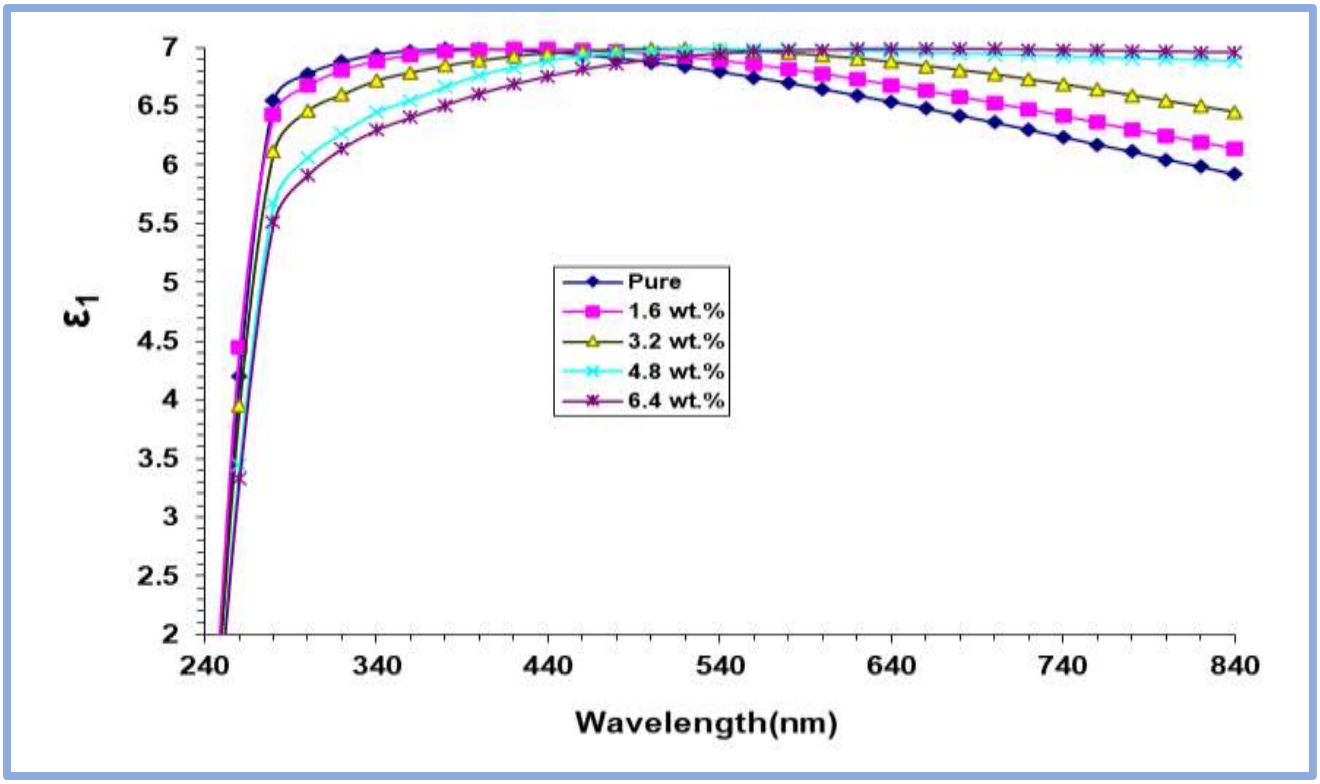

Figure (4.11). Performance of real part of dielectric constant for (PMMA-PEG/Si_3N_4) nanocomposites with wavelength

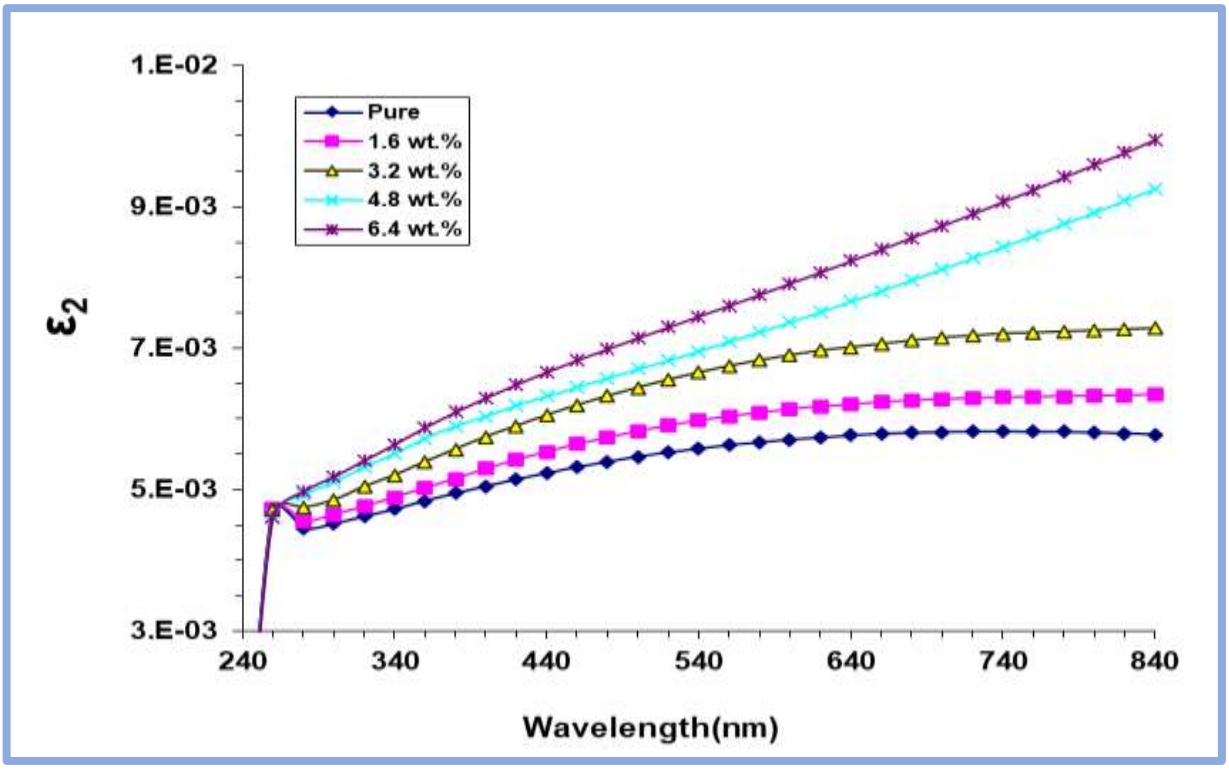

Figure (4.12). Performance of imaginary part of dielectric constant for (PMMA-PEG/Si_3N_4) nano composites with wavelength

4.3.7 Optical conductivity (σ) of (PMMA- PEG/Si_3N_4) nanocomposites

Figure (4.13) shows the variation of optical conductivity for (PMMA-PEG/Si_3N_4) nanocomposites with photon wavelength. As shown in this figure, the optical conductivity of (PMMA-PEG/Si_3N_4) nanocomposites decreased as the wavelength increased,. The increase in optical conductivity at low photon wavelengths is due to the high absorbance of all composite samples in this region, because of the increased excitation charge transfer[123]. Furthermore, the addition of silicon nitride nanoparticles improved the optical conductivity, this phenomenon is associated with the formation of localized levels in the energy gap; which is an increase in the concentration of Si_3N_4 NPS. The density of localized states in the band structure is increased by increasing the nanoparticles. This behavior agrees with the researcher's results [124].

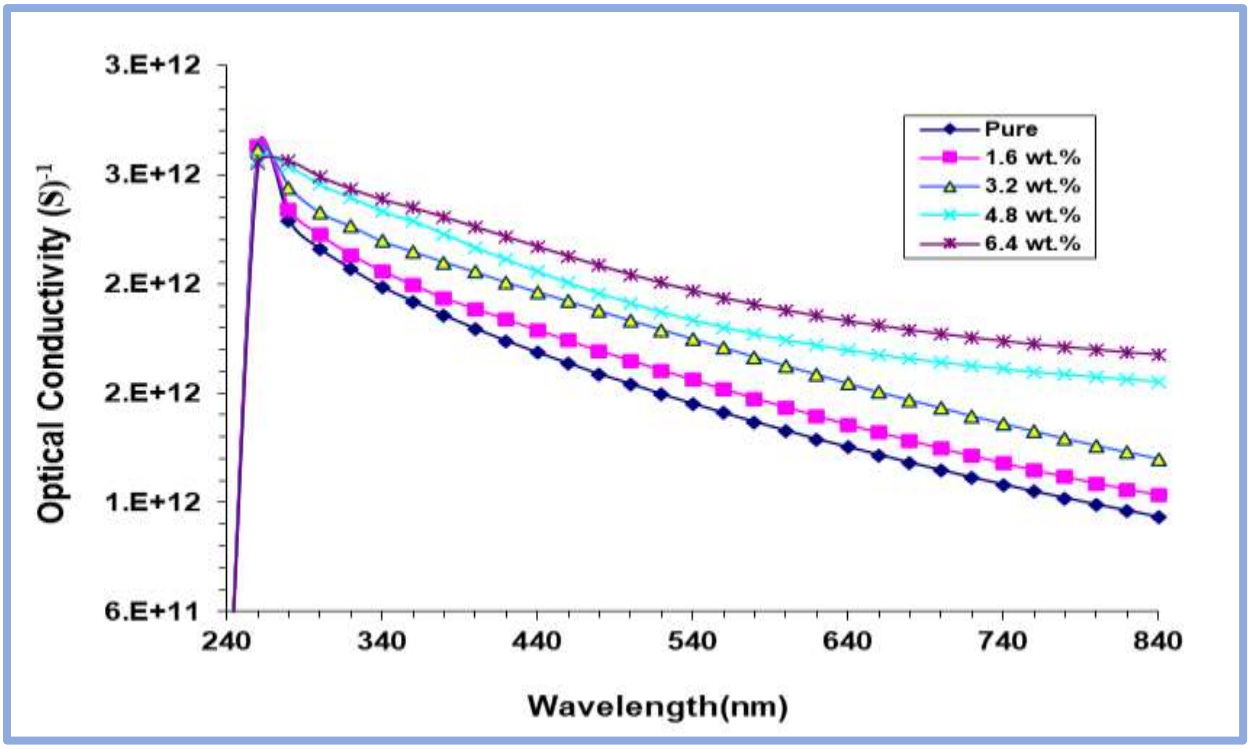

Figure (4.13). Variation of optical conductivity for (PMMA-PEG/Si_3N_4) nanocomposites with wavelength

4.4 The Results of A.C Electrical Properties

4.4.1 Dielectric constant (ε') and dielectric loss (ε'') of (PMMA-PEG/Si_3N_4) Nanocomposites

Figures (4.14) and (4.15) depict the frequency dependence of the dielectric constant and dielectric loss of (PMMA-PEG/Si_3N_4) nanocomposites. The figures show that the dielectric constant ε' and dielectric loss ε" are higher in the lower frequency range and decrease with increasing frequency for all samples, this is due to the Maxwell-Wagner polarization, which causes higher dielectric constants and dielectric losses. This type of polarization is caused by insulator-conductor interfaces. This interfacial polarization is caused by the accumulation of space

charges or dipoles at the interfaces. The space charges have plenty of time to react to the applied electric field in the lower frequency region, whereas in the higher frequency range, changes in the electric field are too quick for the space charges to react and the polarization effect does not exist, hence the increase of the frequency lead to the decrease of the dielectric constant ε' and dielectric loss ε". This behavior agrees with the researchers' results [125,126].

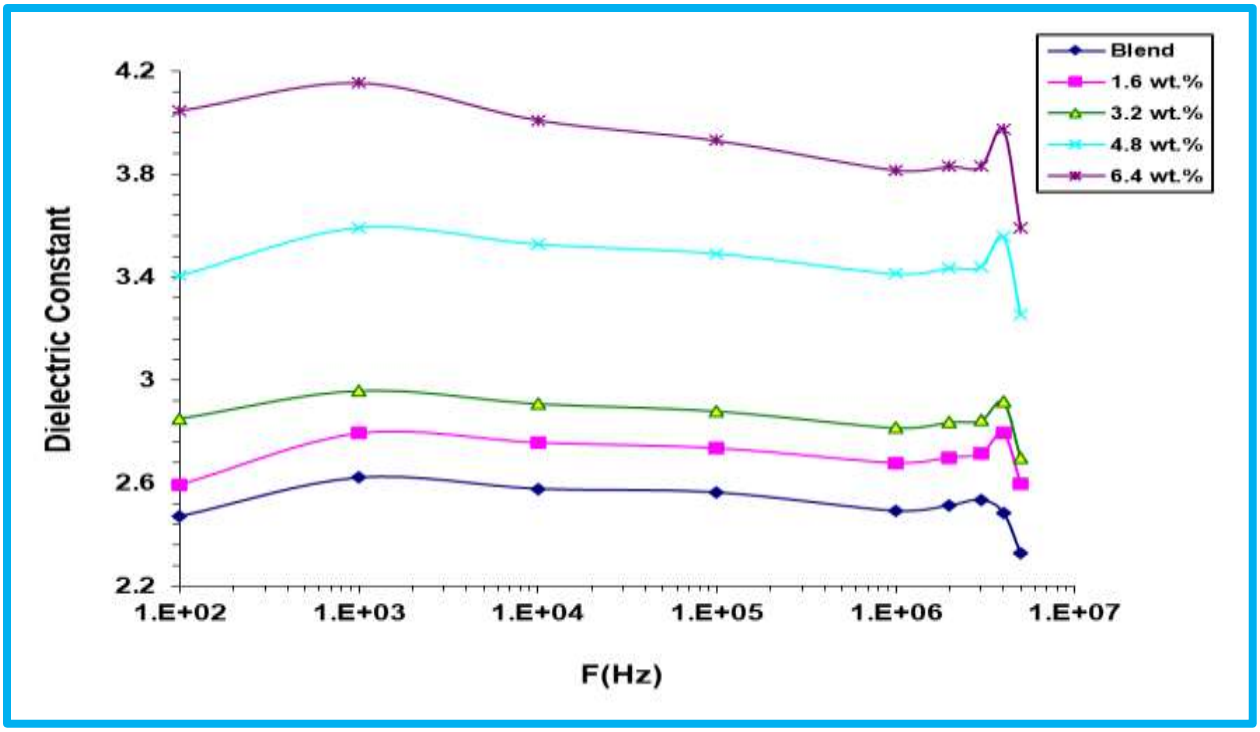

Figure (4.14). Performance of dielectric constant for nanocomposites against frequency

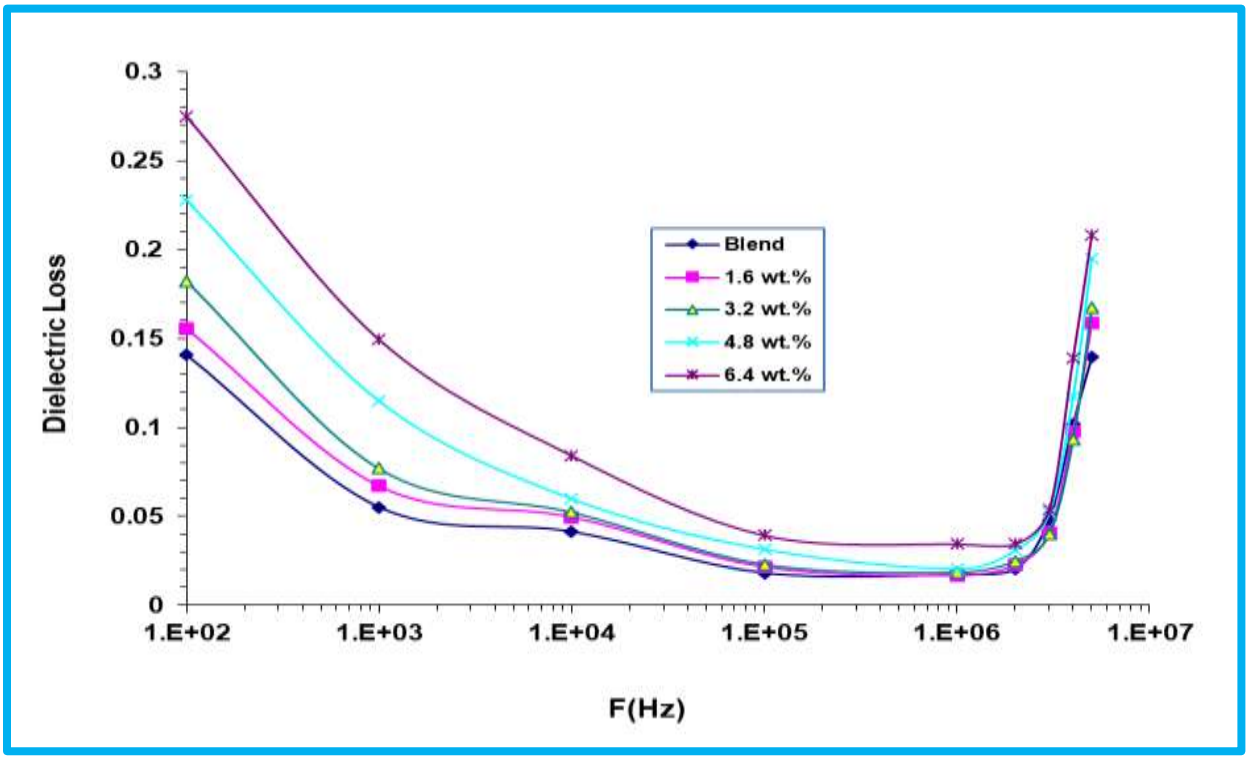

Figure (4.15). Performance of dielectric loss for nanocomposites against frequency

Figures (4.16) and (4.18) show the change of dielectric constant and dielectric loss of (PMMA-PEG) blend with (Si_3N_4) nanoparticles concentration at 100 Hz. The figures show that the dielectric constant and dielectric loss increase with the increase in the Si_3N_4 NPS content. This is due to atomic, ionic, and electronic influences, as well as space charge influences. This behavior agrees with the researcher's results [127]

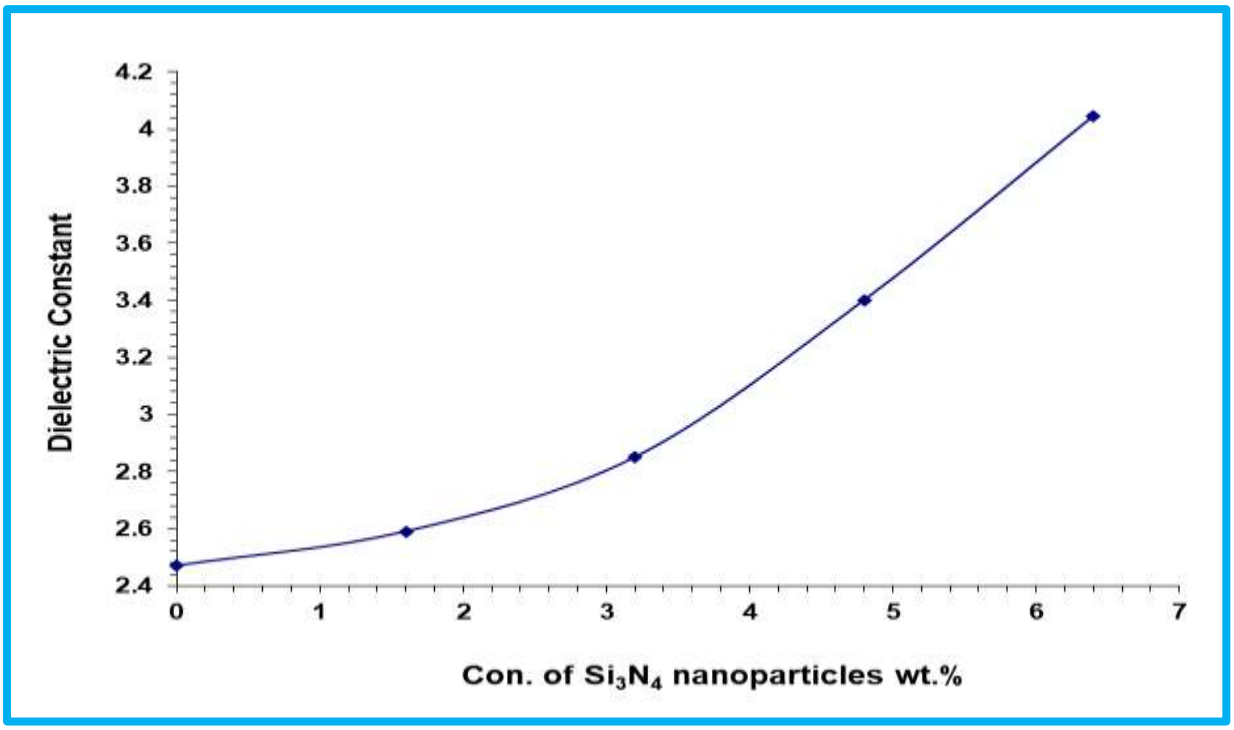

Figure (4.16). Performance of dielectric constant for (PMMA-PEG) blend with concentration of (Si_3N_4) nanoparticles

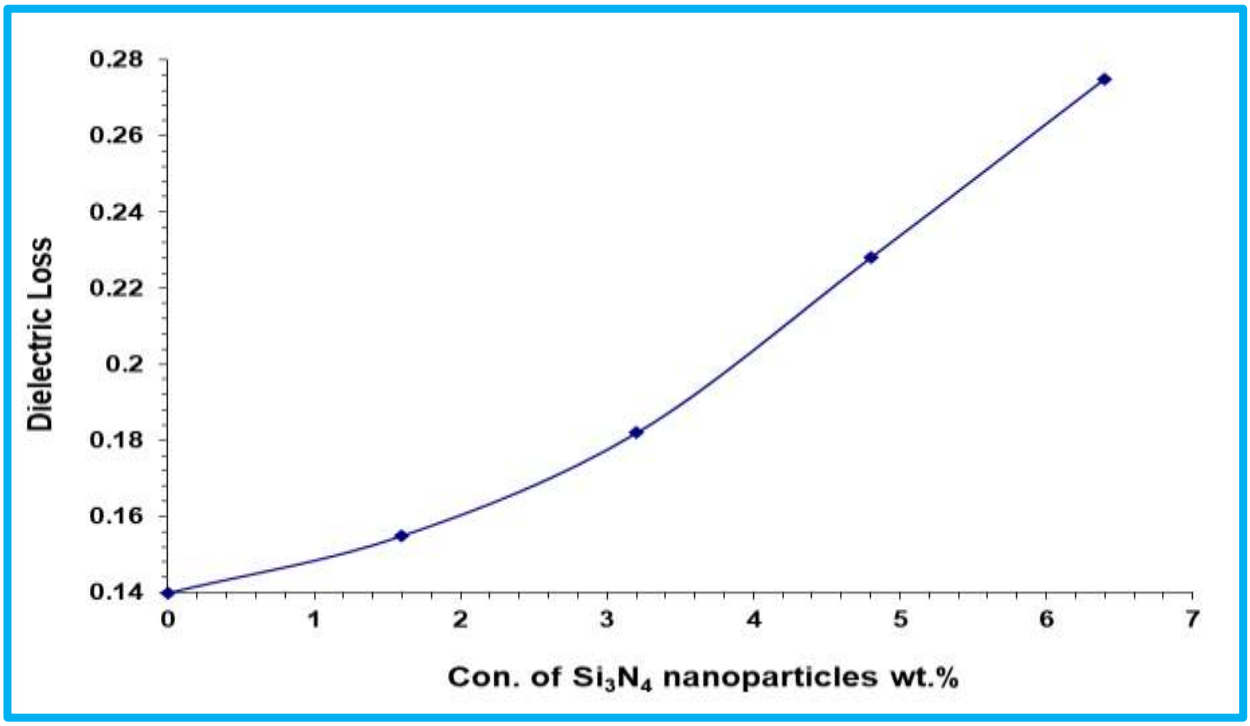

Figure (4.17). Performance of dielectric loss for nanocomposites with concentrations of (Si_3N_4) nanocomposites

4.4.2 A.C Electrical conductivity of (PMMA-PEG/Si_3N_4) nanocomposites

Figure (4.18) shows the variation of A.C electrical conductivity for (PMMA/PEG-Si_3N_4) nanocomposites with electric field frequency at room temperature. Because of space charge polarization, the AC electrical conductivity increases with frequency, as shown in the figure. Both charge carrier stimulation of higher states in the conduction band and low-frequency space charge polarization cause this[128]. The increase of conductivity at high frequencies due to electronic polarization and hopping charge carriers. The two variables that affect A.C. conductivity are the main chain motion and ion movements[129]. Figure (4.19) shows the effect of Si_3N_4 NPS concentration on the electrical conductivity of (PMMA-PEG) blend at 100 Hz. Because the charge carrier density in the polymer medium increases with the concentration of Si_3N_4 nanoparticles, the A.C electrical conductivity increases. '[128,130].

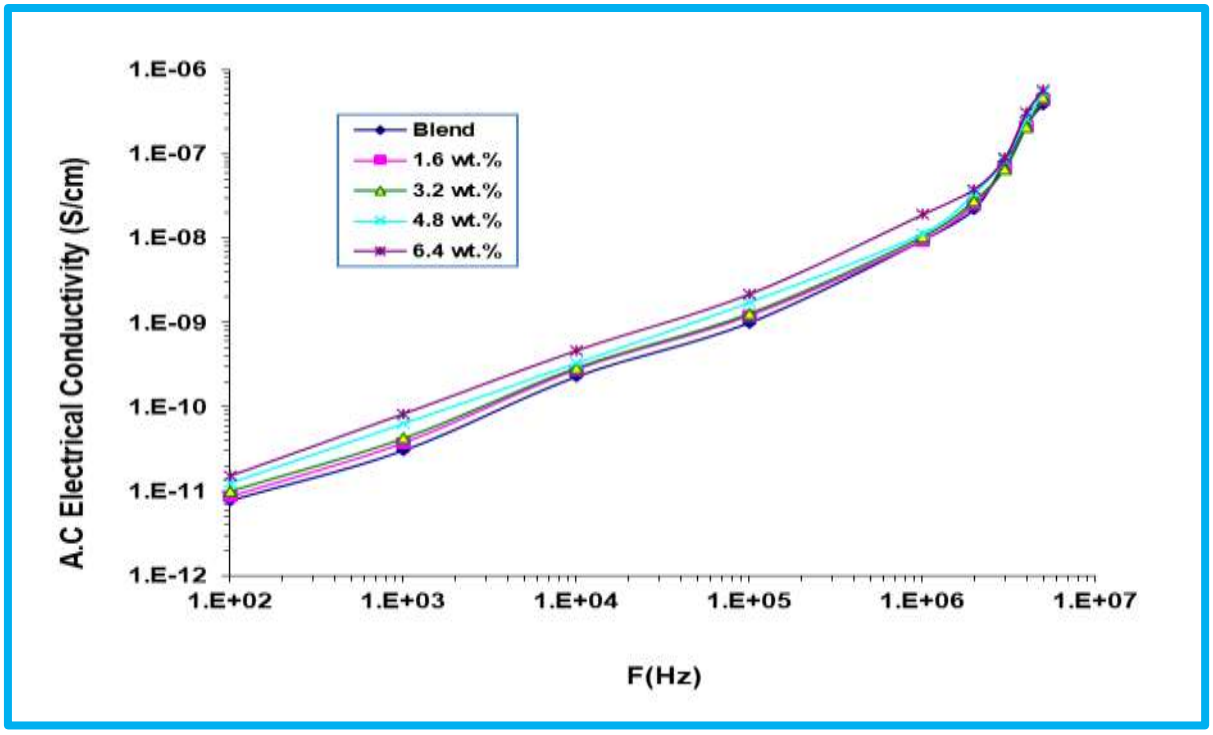

Figure (4.18). Performance of A.C conductivity of (PMMA-PEG/Si_3N_4) nanocomposites with frequency

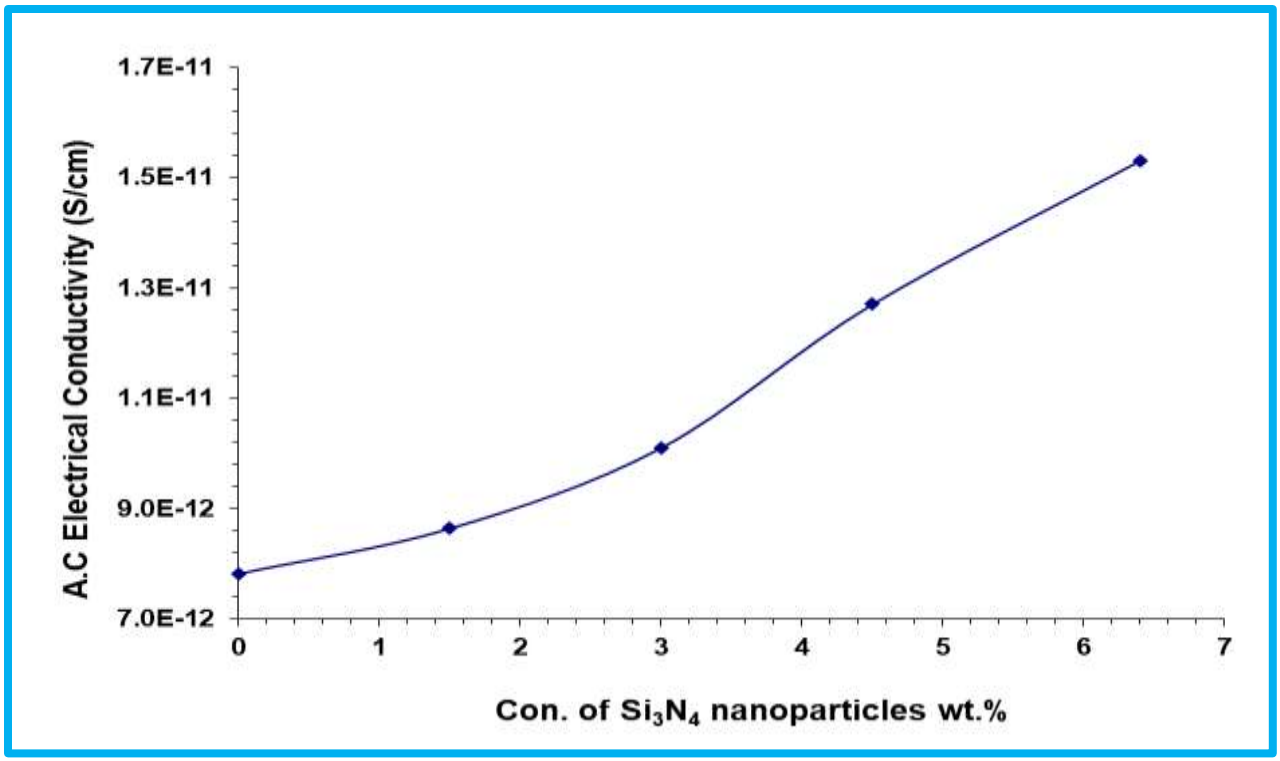

Figure (4.19). Performance of A.C conductivity for (PMMA-PEG) blend with concentrations of (Si_3N_4) nanoparticles

4.5 Application of (PMMA-PEG/Si_3N_4) Nanocomposites for Antibacterial Activity

Figures (4.20) and (4.21) show images of the inhibition zone for Staphylococcus and Escherichia coli. The antibacterial properties of the (PMMA-PEG/Si_3N_4) nanocomposites were tested against gram-positive (Staphylococcus aureus) and gram-negative (Escherichia coli) are presented in figures (4.22) and (4.23). These figures show that the diameter of the inhibition zone increases as the concentration of Si_3N_4 nanoparticles increases[131,132]. The presence of reactive oxygen species (ROS) generated by various nanoparticles may be the cause of nanocomposites' antibacterial activity. The main mechanism causing the antibacterial properties of nanocomposites caused by nanoparticles could be oxidative stress caused by ROS. ROS includes radicals such as superoxide radicals

(O_2), hydroxyl radicals (-OH), hydrogen peroxide (H_2O_2), and singlet oxygen ($_1O_2$) may be the cause of protein and DNA damage in bacteria. The metal oxide could have produced ROS, resulting in the inhibition of most pathogenic bacteria. On the other hand, nanoparticles inside nanocomposites have a negative charge, creating an electromagnetic attraction between the nanoparticles and the microbes. When the attraction is formed, the microbes oxidize and die[133]. Table (4.1) shows the inhibition zone diameter of (PMMA-PEG/Si_3N_4) nanocomposites.

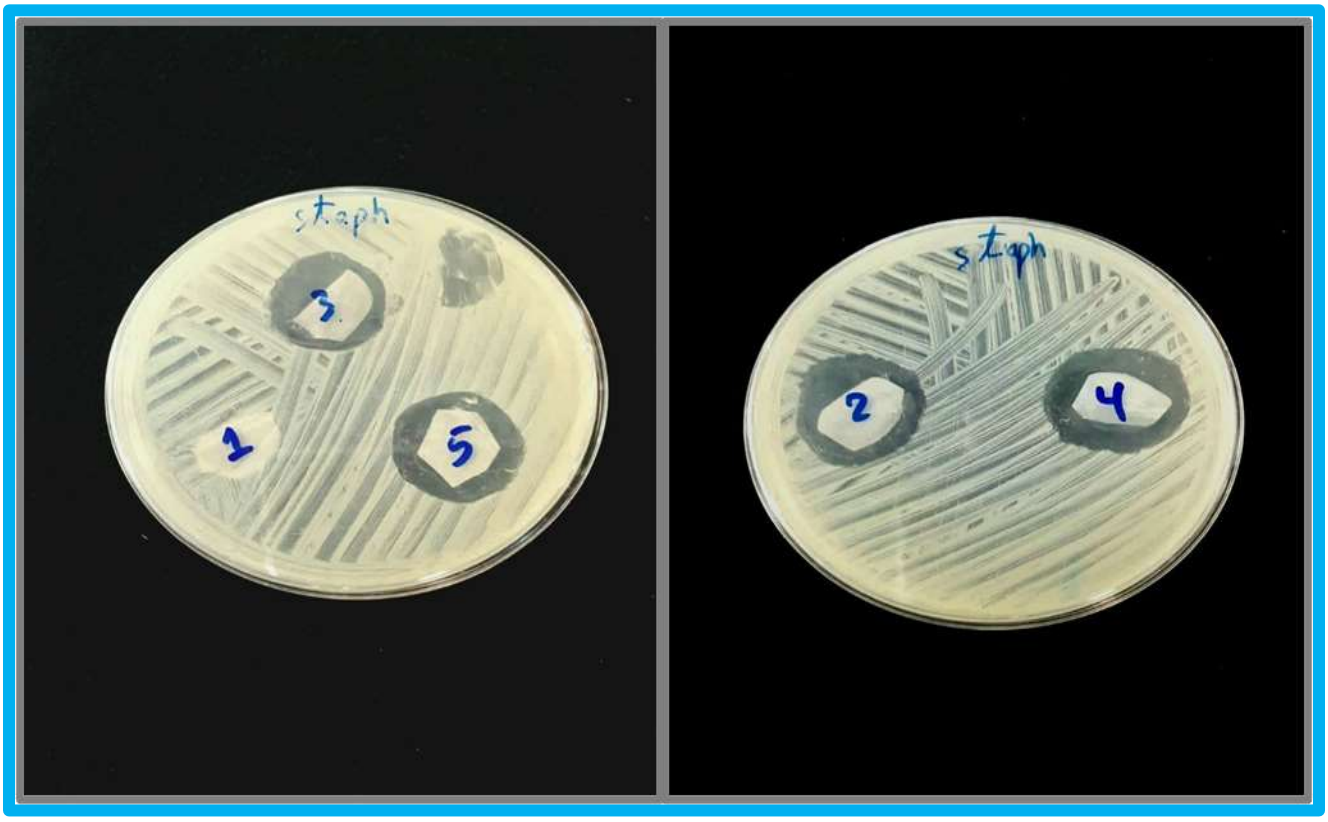

Figure (4.20). Images of inhibition zone for Staphylococcus

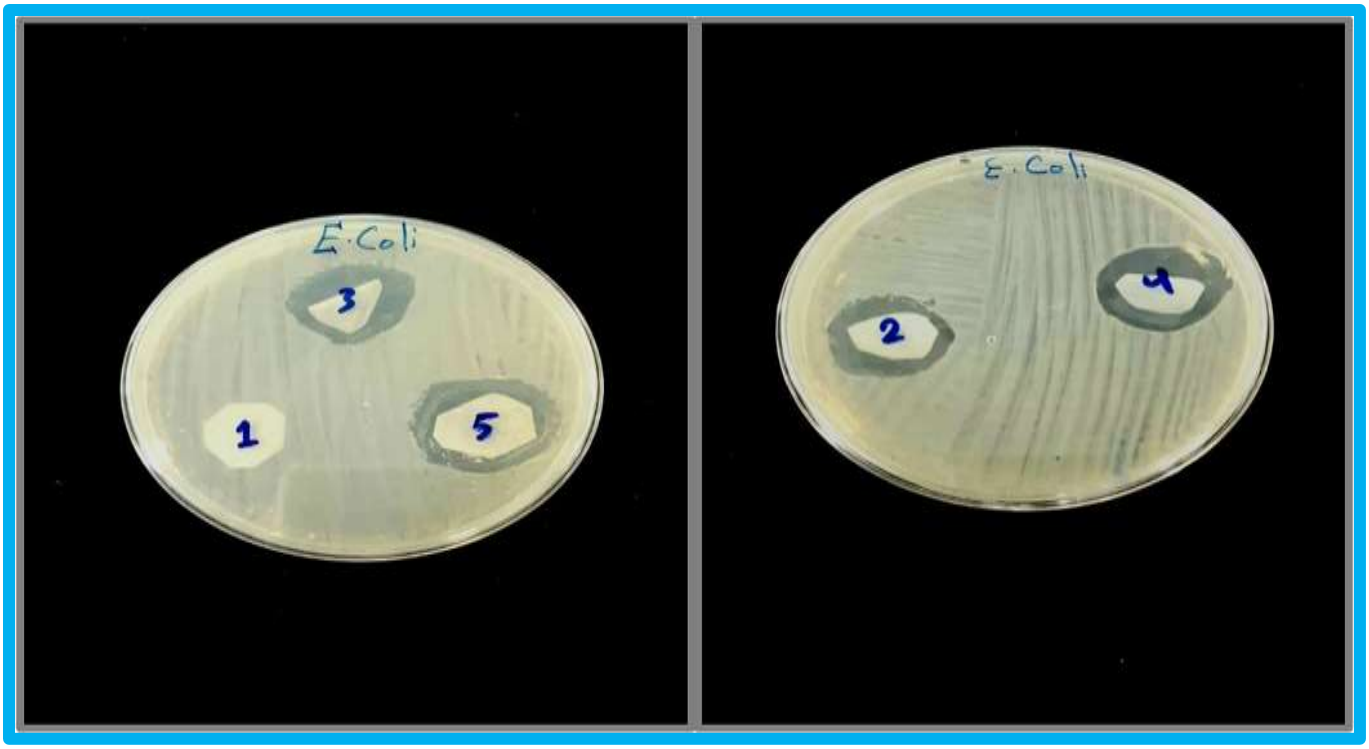

Figure (4.21). Images of inhibition zone for Escherichia coli

Table (4.1). inhibition zone diameter of (PMMA-PEG/Si_3N_4) nanocomposites

concentrations (Si_3N_4) wt%	Inhibitions zone diameter(mm) of Staphylococcus	Inhibitions zone diameter(mm) of Escherichia coli
pure	0	0
1.6	21	19
3.2	22	20
4.8	23	20
6.4	23	22

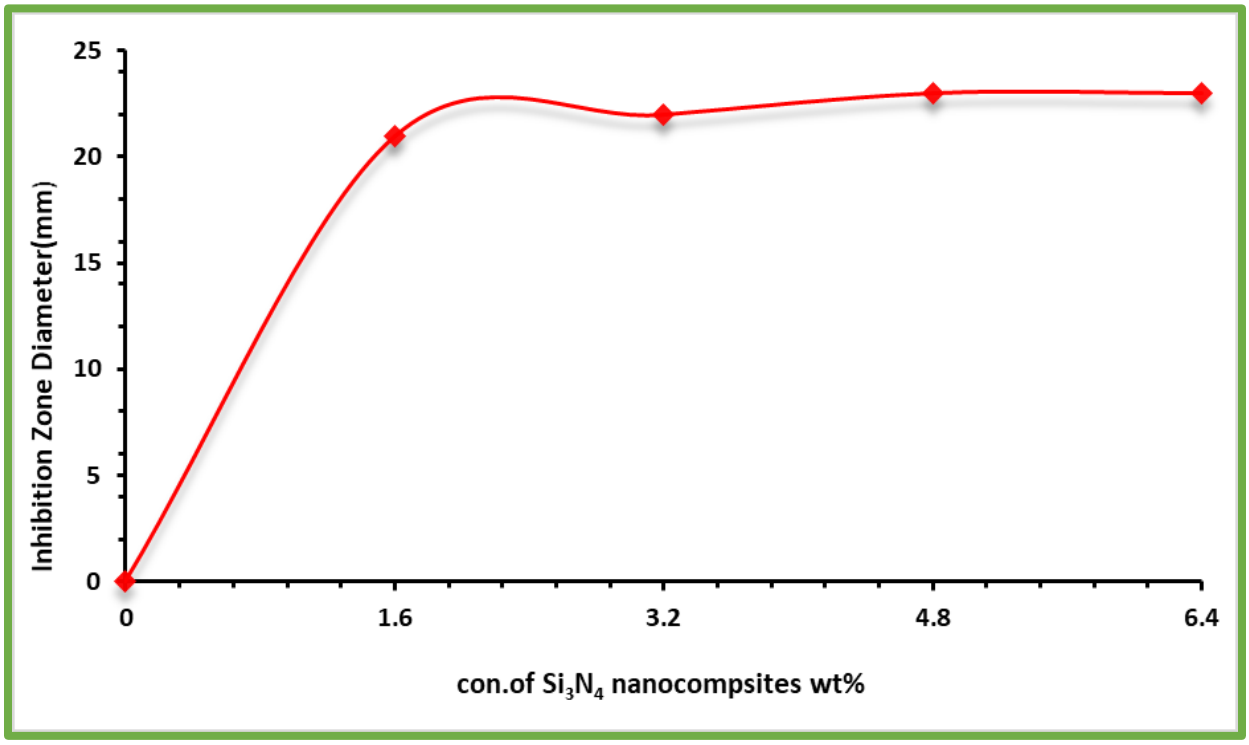

Figure (4.22). Inhibition zone diameter of (PMMA-PEG/Si_3N_4) nanocomposites against Staphylococcus bacterial

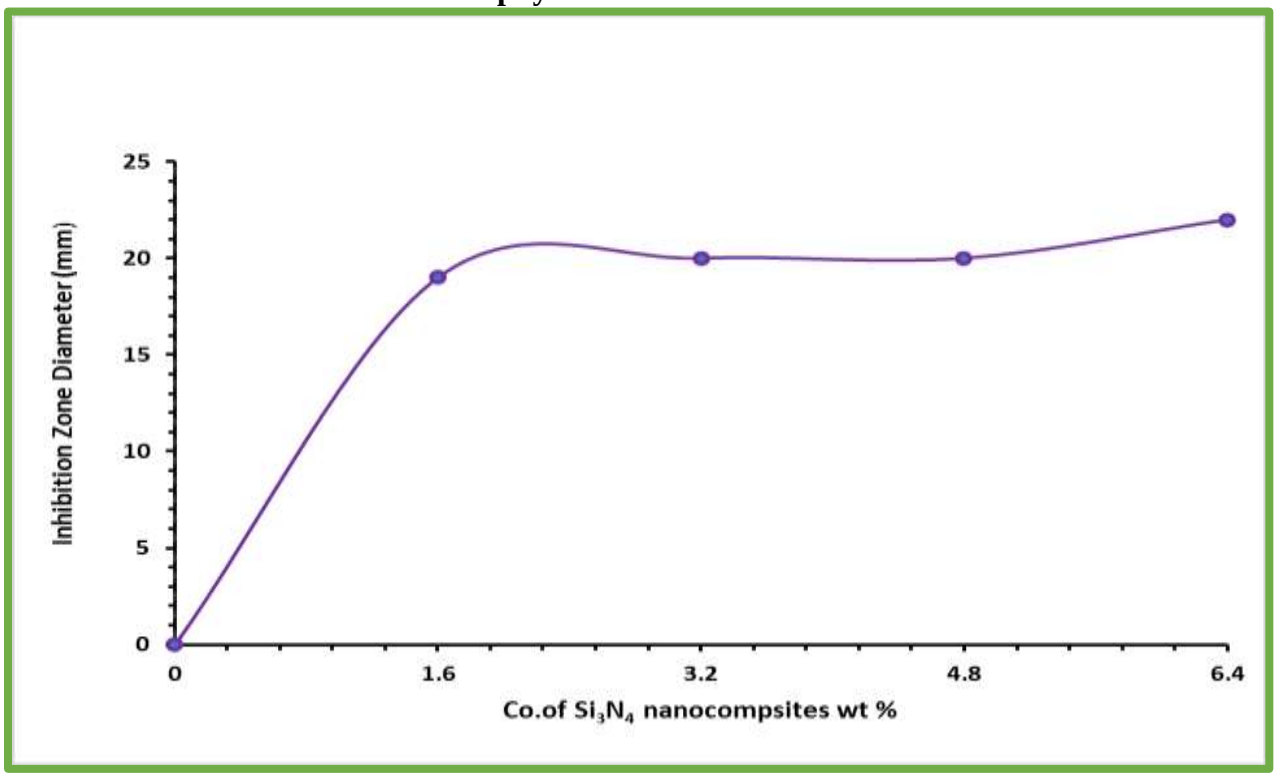

Figure (4.23). Inhibition zone diameter of (PMMA-PEG/Si_3N_4) nanocomposites against Escherichia coli

4.6 Application of (PMMA-PEG/Si_3N_4) Nanocomposites for Gamma Ray Shielding

Figure (4.24) shows the variation of (N/N_0) for the (PMMA-PEG) blend with different concentrations of Si_3N_4 nanoparticles. The transmission radiation decreases with the increasing concentrations of Si_3N_4 nanoparticles, which is attributed to the increase of the attenuation radiation. Figure (4.25) shows the variation of attenuation coefficients of gamma radiation with the Si_3N_4 nanoparticles content ratio. The attenuation coefficients increase with concentrations, due to the absorption or reflection of gamma radiation by nanocomposite shielding materials. The (PMMA-PEG/Si_3N_4) nanocomposites have highest attenuation coefficients, which is due to the high atomic number of Si_3N_4 nanoparticles[134,135].

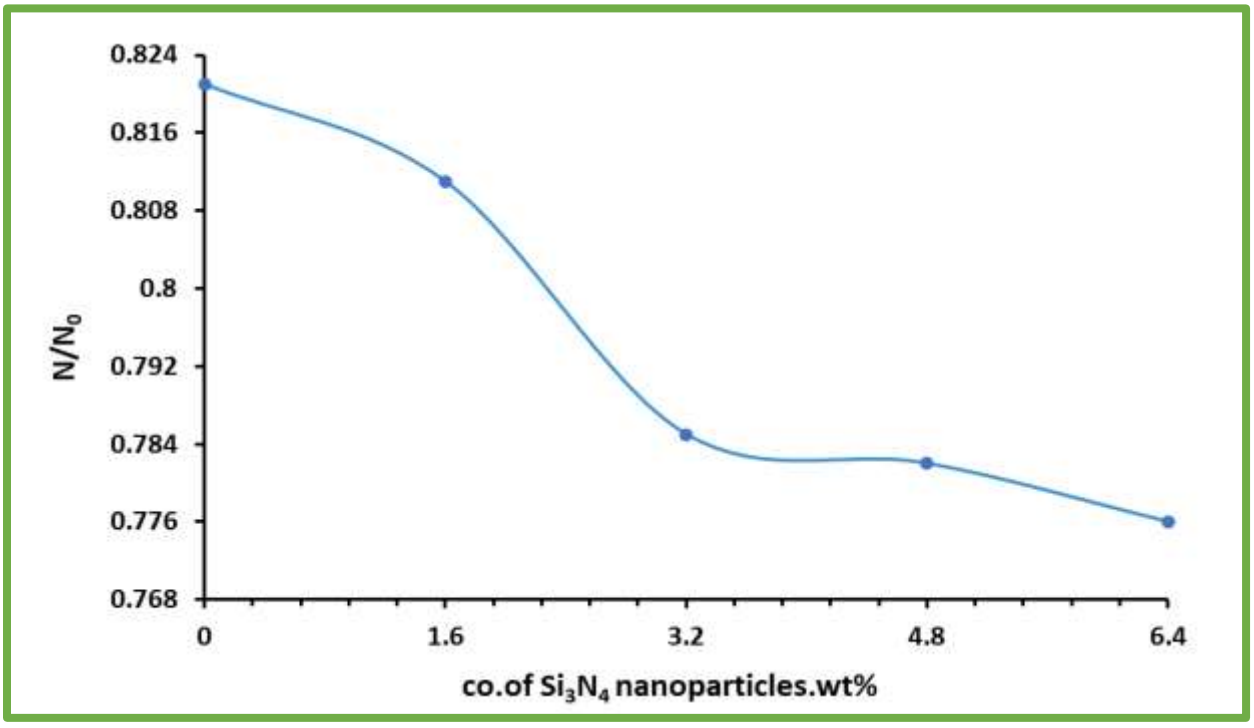

Figure (4.24). Variation of (N/N_0) for (PMMA-PEG/Si_3N_4) nanocomposites

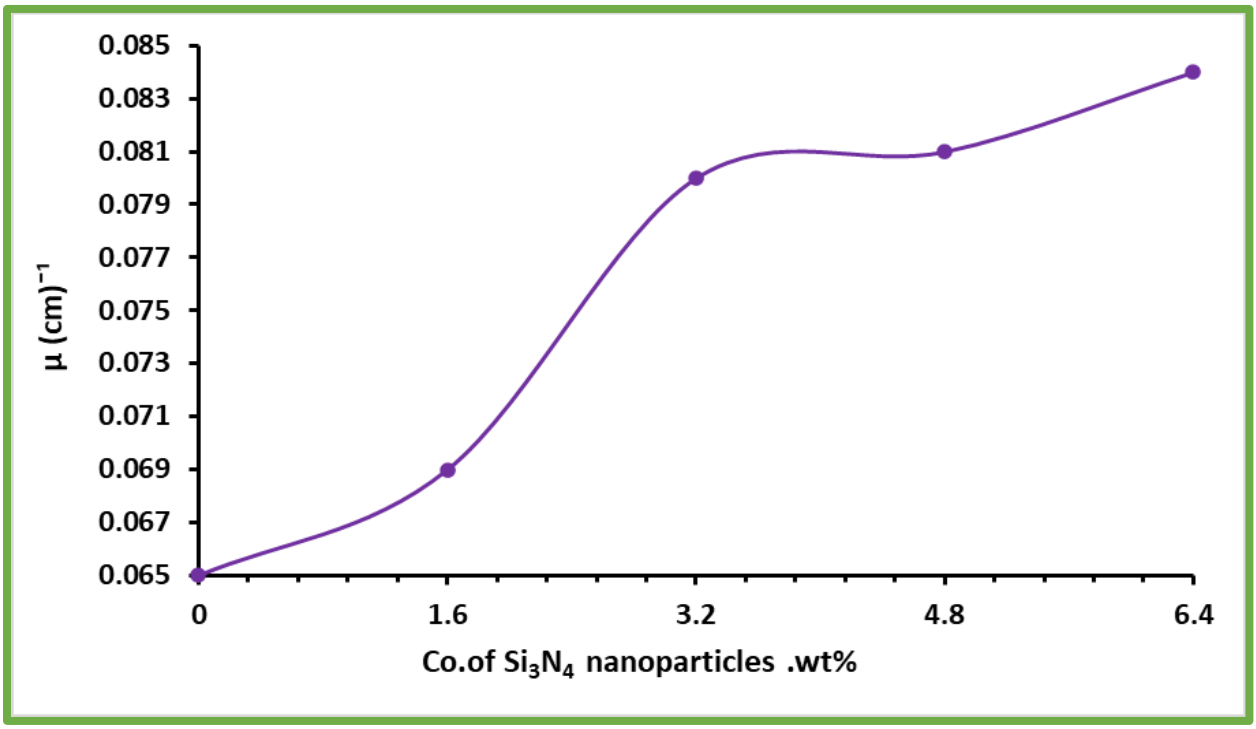

Figure (4.25). Variation of attenuation coefficients of gamma radiation for (PMMA-PEG/Si_3N_4) nanocomposites

4.7 Conclusion

1- The optical microscope images revealed a homogeneous distribution of nanoparticles in the polymer blend and the appearance of network paths as the concentration of silicon nitride, Si3N4, increased. In the surface morphology, the SEM images revealed homogeneity and good distribution.SEM images show that the best distribution of the material and the sample is smooth at a concentration of 4.8 wt%.

The FTIR measurements indicate vibration bands for the polymer blend before and after the addition of silicon nitride (Si_3N_4) nanoparticles and we conclude that the polymer after addition may have formed chains networks of polymer nanocomposites and their effects appeared in electrical and optical properties

2- The absorbance, absorption coefficient (α), extinction coefficient (k), refractive index (n), real and imaginary dielectric constants of (PMMA-PEG/Si_3N_4) nanocomposite increase with increasing the Si_3N_4 nanoparticles concentrations. The Transmittance and energy gap decreases with increasing concentration of the additive. The (PMMA-PEG/Si_3N_4) nanocomposites have high absorbance in the U.V region. These compounds can be used in optical applications and UV-shielding

3- The dielectric constant, the dielectric loss, and A.C electrical conductivity of the (PMMA-PEG/Si_3N_4) nanocomposites decrease with an increase in the frequency of the applied electric field. The dielectric constant, dielectric loss and A.C electrical conductivity of (PMMA-PEG/Si_3N_4) nanocomposites increase with increasing (Si_3N_4) nanoparticles concentrations, which can be useful for different electrinos applications.

4- The results of antibacterial application for (PMMA-PEG/Si_3N_4) nanocomposites showed that the inhibition zone for S. aureus and E. coli increases with increasing concentrations of Si_3N_4 nanoparticles. The attenuation coefficients for gamma radiation increase as the concentrations of nanoparticles increase. The results showed the (PMMA-PEG/Si_3N_4) nanocomposites have good antibacterial activity and high attenuation coefficients at concentration 6.4wt%

4.8 Future Works

1- Studying the D.C electrical properties of (PMMA-PEG/Si_3N_4) nanocomposites.

2- Study of mechanical properties of (PMMA-PEG/Si_3N_4) nanocomposites.

3- Studying the effect of Gamma-ray radiation on optical properties of (PMMA -PEG/Si_3N_4) nanocomposites.

4- Investigating the thermal properties of (PMMA-PEG/Si_3N_4) nanocomposites.

5- Study the effect of temperature on certain physical properties of (PMMA-PEG/Si_3N_4)

REFERENCES

REFERENCES

[1] D. Feldman, "Polymer history," Des. Monomers Polym., vol.11, no.1, pp. 1–15,2008, doi: 10.1163/156855508X292383.

[2] N. S. Alghunaim, "Spectroscopic analysis of PMMA/PVC blends containing CoCl2,"Results Phys, vol. 5,pp. 331–336, 2015,doi:10.1016/j.rinp.2015.11.003

[3] G. Murtaza et al., "Effect of Polyvinyl alcohol on structural and dielectrical properties of polyaniline." Digest Journal of Nanomaterials and Biostructures, vol.14, on. 1, pp.101-108. 2019.

[4] Z. M. Cinan, B. Erol, T. Baskan, S. Mutlu, S. S. Yilmaz, and A. H. Yilmaz, "Gamma irradiation and the radiation shielding characteristics: For the lead oxide doped the crosslinked polystyrene-b-polyethyleneglycol block copolymers and the polystyrene-b-polyethyleneglycol-boron nitride nanocomposites," Polymers (Basel)., vol. 13, no. 19, 2021, doi: 10.3390/polym13193246.

[5] S. Sánchez-Valdes, L. F. Ramos-De Valle, and O. Manero, Polymer Blends, vol. 1. 2013. doi: 10.1002/9781118480793.ch27.

[6] L. Ahmed, B. Zhang, L. C. Hatanaka, and M. S. Mannan, "Application of polymer nanocomposites in the flame retardancy study," J. Loss Prev. Process Ind., vol. 55, pp. 381–391, 2018, doi: 10.1016/j.jlp.2018.07.005.

[7] A. Dorigato, "Recycling of polymer blends," Adv. Ind. Eng. Polym. Res., vol. 4, no. 2, pp. 53–69, 2021, doi: 10.1016/j.aiepr.2021.02.005.

[8] L. H. Gaabour, "Effect of addition of TiO_2 nanoparticles on structural and dielectric properties of polystyrene/polyvinyl chloride polymer blend," AIP Adv., vol. 11, no. 10, 2021, doi: 10.1063/5.0062445.

[9] A. Atta, M. M. Abdelhamied, A. M. Abdelreheem, and M. R. Berber, "Flexible methyl cellulose/polyaniline/silver composite films with enhanced linear and nonlinear optical properties," Polymers (Basel)., vol. 13, no. 8, 2021, doi: 10.3390/polym13081225.

[10] A. S. El-Deeb, M. M. A. Kader, G. M. Nasr, M. A. Ahmed, and E. O. Taha, "Optical Investigation of PVA/$PbTiO_3$ Composite for UV-Protective Approach Applications," pp. 15–31, 2021, doi: 10.3390/ASEC2021.

[11] M. Ali Habeeb, C. Author, B. university, A.-K. J. Al-Bermany, and D. H. Sabeeh, "Effect of polyacrilamide on the rheological and electrical properties of polyethylene glycol," J. Ind. Eng. Res., vol. 1, no. 4, pp. 33–39, 2015.

[12] M. Vamegh, M. Ameri, and S. F. Chavoshian Naeni, "Performance evaluation of fatigue resistance of asphalt mixtures modified by SBR/PP polymer blends and SBS," Constr. Build. Mater., vol. 209, pp. 202–214, 2019, doi: 10.1016/j.conbuildmat.2019.03.111.

[13] C. Koning, M. Van Duin, C. Pagnoulle, and R. Jerome, "Strategies for compatibilization of polymer blends," Prog. Polym. Sci., vol. 23, no. 4, pp. 707–757, 1998, doi: 10.1016/S0079-6700(97)00054-3.

[14] S. Abdul and S. Saood, "Synthesis of Biocompatible Polymer Blend for Drug Delivery in Biomedical Applications," vol. 34, no. 6, pp. 842–851, 2016.

[15] L. M. Robeson, "Polymer Blends: A Comprehensive Review: Chapter 2. Fundamentals of Polymer Blends," Polym. Blends, pp. 11–23, 2007.

[16] D. R. Paul and J. W. Barlow, “Polymer Blends (or Alloys),” J. Macromol. Sci. Part C, vol. 18, no. 1, pp. 109–168, 1980, doi: 10.1080/00222358008080917.

[17] M. Si et al., “Compatibilizing bulk polymer blends by using organoclays,” Macromolecules, vol. 39, no. 14, pp. 4793–4801, 2006, doi: 10.1021/ma060125+.

[18] W. D. Callister, "Materials Science and Engineering An Introduction", New York: John Wiley & Sons, Inc., 2007.

[19] M. Richardon, " Polymer Engineering Composites" , Ist Ed. Applied Science Publishers Ltd. London , (1977) .

[20] R.Kirk and D.F. Othmer , "Encyclopedia of Chemical Technology", John Wileyand Sons, (2012).

[21] A. Shrivastava, "Introduction to Plastics Engineering", in Plastics Design Library, A. B. T.-I. to P. E. Shrivastava, Ed. William Andrew Publishing, 2018, pp. 1–16. doi: https://doi.org/10.1016/B978-0-323-39500-7.00001-0.

[22] R. V. Kulkarni, S. Z. Inamdar, K. K. Das, and M. S. Biradar, "Polysaccharide-based stimuli-sensitive graft copolymers for drug delivery", Elsevier Ltd., 2019. doi: 10.1016/B978-0-08-102553-6.00007-6.

[23] K. Goda, M. S. Sreekala, S. K. Malhotra, K. Joseph, and S. Thomas, "Advances in polymer composites: Biocomposites-state of the art, new challenges, and opportunities", Polym. Compos. Biocomposites, vol. 3, pp. 1–10, 2013, doi: 10.1002/9783527674220.ch1

[24] H. Ishida, S. Campbell, and J. Blackwell, “General approach to nanocomposite preparation,” Chem. Mater., vol. 12, no. 5, pp. 1260–1267, 2000, doi: 10.1021/cm990479y.

[25] B. Ates, S. Koytepe, A. Ulu, C. Gurses, and V. K. Thakur, "Chemistry, structures, and advanced applications of nanocomposites from biorenewable resources," Chem. Rev., vol. 120, no. 17, pp. 9304–9362, 2020, doi: 10.1021/acs.chemrev.9b00553.

[26] J. Musil and J. Vlček, "Magnetron sputtering of hard nanocomposite coatings and their properties," Surf. Coatings Technol., vol. 142–144, pp. 557–566, 2001, doi: 10.1016/S0257-8972(01)01139-2.

[27] Y. H. Kim, D. K. Lee, H. G. Cha, C. W. Kim, and Y. S. Kang, "Synthesis and characterization of antibacterial Ag - SiO2 nanocomposite," J. Phys. Chem. C, vol. 111, no. 9, pp. 3629–3635, 2007, doi: 10.1021/jp068302w.

[28] J. E. Hulla, S. C. Sahu, and A. W. Hayes, "Nanotechnology: History and future," Hum. Exp. Toxicol., vol. 34, no. 12, pp. 1318–1321, 2015, doi: 10.1177/0960327115603588.

[29] P. R. Robinson and C. S. Hsu, "Introduction to petroleum technology," Springer Handbooks, vol. PartF1, pp. 1–83, 2017, doi: 10.1007/978-3-319-49347-3_1.

[30] K. Anil Shenoy, " Effects of multi-wall carbon nanotubes on the mechanical properties of polymeric nanocomposites**,"** PhD Thesis, Wichita State University, 2008.

[31] G. Sahay, D. Y. Alakhova, and A. V. Kabanov, "Endocytosis of nanomedicines," J. Control. Release, vol. 145, no. 3, pp. 182–195, 2010, doi: 10.1016/j.jconrel.2010.01.036.

[32] J. Wang, J. D. Byrne, M. E. Napier, and J. M. Desimone, "More effective nanomedicines through particle design," Small, vol. 7, no. 14, pp. 1919–1931, 2011, doi: 10.1002/smll.201100442.

[33] S. Singh, "Nanomedicine-nanoscale drugs and delivery systems," J. Nanosci. Nanotechnol., vol. 10, no. 12, pp. 7906–7918, 2010, doi: 10.1166/jnn.2010.3617.

[34] B. Y.S. Kim, M.D., J. T. Rutka, and W.C. chan, "Review article," new Engl. J. of Med., vol. 17, no. 2, pp. 121–130, 2010.

[35] A. J. Thorley and T. D. Tetley, "New perspectives in nanomedicine," Pharmacol. Ther., vol. 140, no. 2, pp. 176–185, 2013, doi: 10.1016/j.pharmthera.2013.06.008.

[36] Y. H. Choi and H. K. Han, "Nanomedicines: current status and future perspectives in aspect of drug delivery and pharmacokinetics," J. Pharm. Investig., vol. 48, no. 1, pp. 43–60, 2018, doi: 10.1007/s40005-017-0370-4.

[37] R. Wang, P. S. Billone, and W. M. Mullett, "An overview of Cancer Nanomedicine on the Market and in Clinical Trials," J. Coast. Life Med., vol. 3, no. 6, 2015.

[38] Logothetidis, Stergios, "*Nanomedicine and nanobiotechnology"*, Springer Science & Springer Berlin Heidelberg, pp. 1-26, doi: 10.1007/978-3-642-24181-9_1, 2011.

[39] F. Abolaban and F. Djouider, "Multifunctional nanoparticle platforms for biomedical applications: A review," Dig. J. Nanomater. Biostructures, vol. 15, no. 3, pp. 649–661, 2020.

[40] E. M. Abdelrazek, A. M. Hezma, A. El-khodary, and A. M. Elzayat, "Spectroscopic studies and thermal properties of PCL/PMMA biopolymer blend,"

Egypt. J. Basic Appl. Sci., vol. 3, no. 1, pp. 10–15, 2016, doi: 10.1016/j.ejbas.2015.06.001.

[41] V. K. Thakur, D. Vennerberg, S. A. Madbouly, and M. R. Kessler, "Bio-inspired green surface functionalization of PMMA for multifunctional capacitors," RSC Adv., vol. 4, no. 13, pp. 6677–6684, 2014, doi: 10.1039/c3ra46592f.

[42] A. M. Alsaad, A. A. Ahmad, I. A. Qattan, A. R. El-Ali, S. A. Al Fawares, and Q. M. Al-Bataineh, "Synthesis of optically tunable and thermally stable pmma–pva/cuo nps hybrid nanocomposite thin films," Polymers (Basel)., vol. 13, no. 11,. 2021, doi: 10.3390/polym13111715.

[43] M. S. Zafar, "Prosthodontic applications of polymethyl methacrylate (PMMA): An update," Polymers, vol. 12, no. 10. MDPI AG, pp. 1–35, 01, 2020. doi: 10.3390/polym12102299.

[44] A. Akbari, B. Divband, P. Dehghan, and A. H. Moradi, "Application of nanocomposites based on graphene and metal materials in measurement of nitrate/nitrite in food samples," Biointerface Research in Applied Chemistry, vol. 11, no. 5. AMG Transcend Association, pp. 12769–12783, 15, 2021. doi: 10.33263/BRIAC115.1276912783.

[45] L. Nyangasi, D. Andala, C. Onindo, A. Wanyonyi, and J, Chepngetich, "Processing parameters for electrospinning poly (methyl methacrylate) (PMMA)/titanium isopropoxide composite in a pump-free setup," open Researchafrica.org, vol.27, on, 1, pp. 1-15, 2018.doi: 10.12688/aasopenres.12909.1

[46] U. Ali, K. J. B. A. Karim, and N. A. Buang, "A Review of the Properties and Applications of Poly (Methyl Methacrylate) (PMMA)," Polym. Rev., vol. 55, no. 4, pp. 678–705, 2015, doi: 10.1080/15583724.2015.1031377.

[46] F. W. J. Billmeyer,"Textbook of Polymer Science". John Wiley and Sons, New York.

[47] D. Yamini, G. Devanand Venkatasubbu, J. Kumar, and V. Ramakrishnan, "Raman scattering studies on PEG functionalized hydroxyapatite nanoparticles," Spectrochim. Acta - Part A Mol. Biomol. Spectrosc., vol. 117, pp. 299–303, 2014, doi: 10.1016/j.saa.2013.07.064.

[48] A. A. D'souza and R. Shegokar, "Polyethylene glycol (PEG): a versatile polymer for pharmaceutical applications," Expert Opin. Drug Deliv., vol. 13, no. 9, pp. 1257–1275, 2016, doi: 10.1080/17425247.2016.1182485.

[49] M. Zhang, X. H. Li, Y. D. Gong, N. M. Zhao, and X. F. Zhang, "Properties and biocompatibility of chitosan films modified by blending with PEG," Biomaterials, vol. 23, no. 13, pp. 2641–2648, 2002, doi: 10.1016/S0142-9612(01)00403-3.

[50] B. Mohammed, H. Ahmed, and A. Hashim, "Studies on Polymer Blend / $BaTiO_3$ Nanocomposites for Industrial and Biological Applications," no. October, 2022, doi: 10.22587/jasr.2022.18.2.1.

[51] A. Spietelun, M. Pilarczyk, A. Kloskowski, and J. Namieśnik, "Polyethylene glycol-coated solid-phase microextraction fibres for the extraction of polar analytes - A review," Talanta, vol. 87, no. 1, pp. 1–7, 2011, doi: 10.1016/j.talanta.2011.09.061.

[52] M. Fukuhara, K. Fukazawa, and A. Fukawa, "Physical properties and cutting performance of silicon nitride ceramic," Wear, vol. 102, no. 3, pp. 195–210, 1985, doi: 10.1016/0043-1648(85)90218-2.

[53] A. J. Moulson, “Reaction-bonded silicon nitride: its formation and properties,” J. Mater. Sci., vol. 14, no. 5, pp. 1017–1051, 1979, doi: 10.1007/BF00561287.

[54] F. de Brito Mota, J. Justo, and A. Fazzio, “Structural properties of amorphous silicon nitride,” Phys. Rev. B - Condens. Matter Mater. Phys., vol. 58, no. 13, pp. 8323–8328, 1998, doi: 10.1103/PhysRevB.58.8323.

[55] G. Ziegler, J. Heinrich, and G. Wötting, “Relationships between processing, microstructure and properties of dense and reaction-bonded silicon nitride,” J. Mater. Sci., vol. 22, no. 9, pp. 3041–3086, 1987, doi: 10.1007/BF01161167.

[56] Z. Krstic and V. D. Krstic, “Silicon nitride: The engineering material of the future,” J. Mater. Sci., vol. 47, no. 2, pp. 535–552, 2012, doi: 10.1007/s10853-011-5942-5.

[57] V. M. Bermudez and F. K. Perkins, “Preparation and properties of clean Si 3 N 4 surfaces,” Appl. Surf. Sci., vol. 235, no. 4, pp. 406–419, Aug. 2004, doi: 10.1016/j.apsusc.2004.02.065.

[58] V. Mohanavel and M. Ravichandran, “Optimization of Parameters to Improve the Properties of AA7178/Si3N4 Composites Employing Taguchi Approach,” Silicon, vol. 14, no. 4, pp. 1381–1394, 2022, doi: 10.1007/s12633-020-00917-0.

[59] B. H. Rabee, F. Z. Razooqi, and M. H. Shinen, “Investigation of optical properties for (PVA-PEG-Ag) polymer nanocomposites films,” Chem. Mater. Res., vol. 7, pp. 103–109, 2015.

[60] R. G. Kadhim, “Study the Electrical and Structural Properties of (PMMA-TiO 2) nanocomposites,” vol. 7, no. 9, pp. 37–49, 2015.

[61] B. H. Rabee and B. A. Al-Kareem, "Study of optical properties of (PMMA-CuO) nanocomposites," Int. J. Sci. Res, vol. 5, no. 4, 2016.

[62] M. A. Habeeb, "Enhancement of Dielectric and Optical Properties of (PVA-PAA-PEG) Blend-Yttrium Oxide Nanoparticle for Biomedical Applications," Mater. Focus, vol. 5, no. 6, pp. 550–555, 2016, doi: 10.1166/mat.2016.1359.

[63] H. M. Shanshool, M. Yahaya, W. M. M. Yunus, and I. Y. Abdullah, "Investigation of energy band gap in polymer/ZnO nanocomposites," J. Mater. Sci. Mater. Electron., vol. 27, no. 9, pp. 9804–9811, 2016, doi: 10.1007/s10854-016-5046-8.

[64] H. M. Mohssin, "Investigation of optical properties for (PVA-PEG-Ag) polymer nanocomposites films," Int. J. Eng. Res. Technol.(IJERT), vol. 6, no. 7, pp. 164–170, 2017.

[65] R. Agool, K. J. Kadhim, and A. Hashim, "Synthesis of (PVA–PEG–PVP–ZrO2) nanocomposites for energy release and gamma shielding applications," Int. J. Plast. Technol., vol. 21, no. 2, pp. 444–453, 2017, doi: 10.1007/s12588-017-9196-1.

[66] S. Devikala, P. Kamaraj, and M. Arthanareeswari, "AC conductivity studies of PMMA/TiO2 composites," Mater. Today Proc., vol. 5, no. 2, pp. 8678–8682, 2018, doi: 10.1016/j.matpr.2017.12.293.

[67] K. Kannan, L. Guru Prasad, S. Agilan, and N. Muthukumarasamy, "Investigations on Ag2S/PVA-PEG polymer nanocomposites: An effectual nonlinear optical material," Optik (Stuttg)., vol. 170, no. May, pp. 10–16, 2018, doi: 10.1016/j.ijleo.2018.05.078.

[68] M. H. Suhail, "Structural and optical properties for PVA- PEG-MnCl2 composites," Iraqi J. Phys., vol. 15, no. 32, pp. 99–113, 2019, doi: 10.30723/ijp.v15i32.160.

[69] M. Bafna, A. Kumar Gupta, and R. K. Khanna, "Effect of potassium chromate nanoparticles on the optical properties of poly (methyl methacrylate) (PMMA) films," Mater. Today Proc., vol. 10, pp. 38–45, 2019, doi: 10.1016/j.matpr.2019.02.186.

[70] P. Rani, M. B. Ahamed, and K. Deshmukh, "Dielectric and electromagnetic interference shielding properties of carbon black nanoparticles reinforced PVA/PEG blend nanocomposite films," Mater. Res. Express, vol. 7, no. 6, 2020, doi: 10.1088/2053-1591/ab9853.

[71] J. Q. M. Almarashi and M. H. Abdel-Kader, "Exploring Nano-sulfide Enhancements on the Optical, Structural and Thermal Properties of Polymeric Nanocomposites," J. Inorg. Organomet. Polym. Mater., vol. 30, no. 8, pp. 3230–3240, 2020, doi: 10.1007/s10904-020-01482-0.

[72] P. Dhatarwal, S. Choudhary, and R. J. Sengwa, "Dielectric and optical properties of alumina and silica nanoparticles dispersed poly(methyl methacrylate) matrix-based nanocomposites for advanced polymer technologies," J. Polym. Res., vol. 28, no. 2, pp. 5–9, 2021, doi: 10.1007/s10965-020-02406-9.

[73] S. S. Al-Abbas et al., "Influence of the polymer molecular weights on the electrical properties of Poly(vinyl alcohol) - Poly(ethylene glycols)/Graphene oxide nanocomposites," Mater. Today Proc., vol. 42, pp. 2469–2474, 2021, doi: 10.1016/j.matpr.2020.12.565.

[74] Z. K. Heiba, M. Bakr Mohamed, and S. I. Ahmed, "Exploring the physical properties of PVA/PEG polymeric material upon doping with nano gadolinium

oxide: Exploring the physical properties of PVA/PEG polymeric material," Alexandria Eng. J., vol. 61, no. 5, pp. 3375–3383, May 2022, doi: 10.1016/j.aej.2021.08.051.

[75] F. S. Jaber, A. Hashim, and H. M. Abduljalil, "Exploring the Design and Spectroscopic Characteristics of PVA/Si3N4/SiBr4 New Structures for Electronics and Optics Devices," Silicon, pp. 1–11, 2022,doi: 10.1007/s12633-022-02000-2

[76] A. Abdullah and A. Mohammed, "Scanning Electron Microscopy (SEM): A Review," Proc. 2018 Int. Conf. Hydraul. Pneum. - HERVEX, pp. 77–85, 2019.

[77] M. A. Mohamed, J. Jaafar, A. F. Ismail, M. H. D. Othman, and M. A. Rahman, Fourier Transform Infrared (FTIR) Spectroscopy. Elsevier B.V., 2017. doi: 10.1016/B978-0-444-63776-5.00001-2.

[78] A. S. Hassanien and A. A. Akl, "Optical characteristics of iron oxide thin films prepared by spray pyrolysis technique at different substrate temperatures," Appl. Phys. A Mater. Sci. Process., vol. 124, no. 11, pp. 1–16, 2018, doi: 10.1007/s00339-018-2180-6.

[79] K. H. H. Al-Attiyah, A. Hashim, and S. F. Obaid, "Fabrication of novel (carboxy methyl cellulose–polyvinylpyrrolidone–polyvinyl alcohol)/lead oxide nanoparticles: structural and optical properties for gamma rays shielding applications," Int. J. Plast. Technol., vol. 23, no. 1, pp. 39–45, 2019, doi: 10.1007/s12588-019-09228-5.

[80] S. M. Hassan, "Optical properties for prepared polyaniline / Ferro fluid nano composites," Iraqi J. Phys., vol. 14, no. 31, pp. 161–168, 2019, doi: 10.30723/ijp.v14i31.183.

[81] O. K. Abdali and O. Abdulazeez, "Optical and Dielectrical Properties of (PEG-CMC) Films Prepared by Drop Casting Method," Wsn, vol. 46, pp. 189–203, 2016,

[82] H. Singh, T. Singh, and J. Sharma, "Review on optical, structural and electrical properties of ZnTe thin films: effect of deposition techniques, annealing and doping," ISSS J. Micro Smart Syst., vol. 7, no. 2, pp. 123–143, 2018, doi: 10.1007/s41683-018-0026-2.

[83] M. Q. Kareem, S. A. Hassan, and M. M. Ameen, "Doping Effect ((COCl 2 . 6H 2 O) & (CuCl 2 . 6H 2 O))(2 %) w / v on Optical Energy gap of (GA / PVA) composite films gap of (GA / PVA) composite films," vol.20, no. 4, pp. 2–8, 2015.

[84] B. H. Rabee and N. A. Hadi, "Study the effect of nano-Mgo on the optical properties of (PVA-PEG-Mgo) Nanocomposites," IJERT, vol. 3, no. 6, pp. 2257–2260, 2014.

[85] R. M. Yas, "Gamma radiation induced changes in the optical properties of CdTe thin films for dosimetric purposes," Iraqi J. Phys., vol. 10, no. 17, pp. 71–76, 2012.

[86] D. Sahoo et al., "Optimization of linear and nonlinear optical parameters in As40Se60 film by annealing at different temperature," Optik (Stuttg)., vol. 219, no. July, p. 165286, 2020, doi: 10.1016/j.ijleo.2020.165286.

[87] T. S. Soliman and S. A. Vshivkov, "Effect of Fe nanoparticles on the structure and optical properties of polyvinyl alcohol nanocomposite films," J. Non. Cryst. Solids, vol. 519, no. May, 2019, doi: 10.1016/j.jnoncrysol.2019.05.028.

[88] R. G. Kadhim, "Study of Some Optical Properties of Polystyrene - Copper Nanocomposite Films," World Sci. News, vol. 30, pp. 14–25, 2016.

[89] M. Abbas, M. Abdallah, and T. Alwan, "Optical characterization of nickel doped poly vinyl alcohol films," SOP Trans. Phys. Chem., vol. 1, no. 2, pp. 1–9, 2014, doi: 10.15764/pche.2014.02001.

[90] M. H. Shinen, S. A. A. Alsaati, and F. Z. Razooqi, "Preparation of high transmittance TiO2 thin films by sol-gel technique as antireflection coating," J. Phys. Conf. Ser., vol. 1032, no. 1, 2018, doi: 10.1088/1742-6596/1032/1/012018.

[91] S. M. H., "Optical properties for prepared polyvinyl alcohol/ polyaniline/ ZnO nanocomposites," Iraqi J. Phys., vol. 16, no. 36, pp. 181–189, 2018, doi: 10.30723/ijp.v16i36.42**.**

[92] T. A. Taha, "Optical properties of PVC/Al2O3 nanocomposite films," Polym. Bull., vol. 76, no. 2, pp. 903–918, 2019, doi: 10.1007/s00289-018-2417-8.

[93] H. I. Jafar, N. A. Ali, and A. Shawky, "Study of A . C Electrical Properties of Aluminum – Epoxy Composites," vol. 14, no. 3, pp. 77–82, 2011.

[94] P. Barber et al., Polymer composite and nanocomposite dielectric materials for pulse power energy storage, vol. 2, no. 4. 2009. doi: 10.3390/ma2041697.

[95] A. Hashim, I. R. Agool, and K. J. Kadhim, "Novel of (polymer blend-Fe3O4) magnetic nanocomposites: preparation and characterization for thermal energy storage and release, gamma ray shielding, antibacterial activity and humidity sensors applications," J. Mater. Sci. Mater. Electron., vol. 29, no. 12, pp. 10369–10394, 2018, doi: 10.1007/s10854-018-9095-z.

[96] R. G. Kadhim, M. A. Habeeb, and Q. M. Jebur, "Dielectric and optical properties for (poly vinyl alcohol-carboxymethyl cellulose–copper oxide)

nanocomposites and their applications," J. Chem. Pharm. Sci., vol. 10, no. 1, pp. 732–739, 2017.

[97] H. A. Jalil Hussien, R. G. Kadhim, and A. Hashim, "Investigation of Structural and Dielectric Properties of (Polymer Blend/Oxides Nanoparticles) for Pressure Sensors," J. Phys. Conf. Ser., vol. 1818, no. 1, 2021, doi: 10.1088/1742-6596/1818/1/012187.

[98] M. Sabu, E. Bementa, Y. Jaya Vinse Ruban, and S. Ginil Mon, "A novel analysis of the dielectric properties of hybrid epoxy composites," Adv. Compos. Hybrid Mater., vol. 3, no. 3, pp. 325–335, 2020, doi: 10.1007/s42114-020-00166-0.

[99] R. Singh, M. S. Smitha, and S. P. Singh, "The role of nanotechnology in combating multi-drug resistant bacteria," J. Nanosci. Nanotechnol., vol. 14, no. 7, pp. 4745–4756, 2014, doi: 10.1166/jnn.2014.9527.

[100] Yin, Iris Xiaoxue, et al. "The antibacterial mechanism of silver nanoparticles and its application in dentistry." *International journal of nanomedicine* :pp. 2555-2562. (2020), doi: 10.2147/IJN.S246764.

[101] M. K. Roy, R. G. Mahloniya, J. Bajpai, and A. K. Bajpai, "Spectroscopic and morphological evaluation of gamma radiation irradiated polypyrole based nanocomposites," Adv. Mater. Lett., vol. 3, no. 5, pp. 426–432, 2012, doi: 10.5185/amlett.2012.6373.

[102] L. M. Chaudhari and R. Nathuram, "Absorption Coefficient of Polymers (Polyvinyl Alcohol) by Using Gamma Energy of 0.39 MeV," Bulg. J. Phys, vol. 37, no. 1, pp. 232–240, 2010, [Online]. Available: http://www.bjp-bg.com/papers/bjp2010_4_232-240.pdf

[103] M. Moharram El-Toony and I. Bashter, "Application of Epoxy/ Pb 3 O 4 Composite for Gamma Ray Shielding," vol. 46, no. 2, pp. 226–233, 2013.

[104] S. M. Badawy and A. A. Abd El-Latif, "Synthesis and characterizations of magnetite nanocomposite films for radiation shielding," Polym. Compos., vol. 38, no. 5, pp. 974–980, 2017, doi: 10.1002/pc.23660.

[105] H. Ahmed, A. Hashim, and H. M. Abduljalil, "Analysis of structural, electrical and electronic properties of (polymer nanocomposites/ silicon carbide) for antibacterial application," Egypt. J. Chem., vol. 62, no. 4, pp. 1167–1176, 2019, doi: 10.21608/EJCHEM.2019.6241.1522.

[106] B. H. Rabee and R. Haider, "The effect of adding Ag nanoparticles on the electrical properties (AC) of the PMMA-SPO-PS blend," in Journal of Physics: Conference Series, 2021, vol. 1973, no. 1, p. 12102.

[107] Z. M. Jawad and K. H. Abass, "Structural and Dispersion Parameters of PVA-PAAm-CuNW for Optical and antibacterial applications," HIV Nurs., vol. 22, no. 2, pp. 842–848, 2022.

[108] S. Kadhum Alsaedi, S. Salih, and F. Hashim, "Preparation and Characterization of Polymer Blend and Nano Composite Materials Based on PMMA Used for Bone Tissue Regeneration," Eng. Technol. J., vol. 38, no. 4A, pp. 501–509, 2020, doi: 10.30684/etj.v38i4a.383.

[109] S. B. Balakrishnan, M. Alam, N. Ahmad, M. Govindasamy, S. Kuppu, and S. Thambusamy, "Electrospinning nanofibrous graft preparation and wound healing studies using ZnO nanoparticles and glucosamine loaded with poly(methyl methacrylate)/polyethylene glycol," New J. Chem., vol. 45, no. 18, pp. 7987–7998, 2021, doi: 10.1039/d0nj05409g.

[110] Chen, M., Zhou, W., Zhang, J., & Chen, Q. Dielectric property and space charge behavior of polyimide/silicon nitride nanocomposite films. *Polymers*, vol.*12*, *no* 2, (2020), doi:10.3390/polym12020322.

[111] S. A. Salman, N. A. Bakr, and M. R. Jwameer, "Synthesis and Study of Some Optical and Thermal Properties of (PVA-CuCl) Films," Res. J. Chem. Sci. ISSN, vol. 5, pp. 25- 32, 2015.

[112] A. D. Acharya, B. Sarwan, I. A. Malik, and Y. Ahmad, "Optical properties of NiO : PVA thin films Optical Properties of NiO : PVA Thin Films," vol. 020006, no.1, 2019.

[113] H. Neama and N. Al-khegani, "The Effect of Ferrous Chloride (FeCl 2) on Some Optical Properties of Polystyrene," vol. 5, no.2, pp. 161–166, 2014.

[114] M. Matamoros-Ambrocio, E. Sánchez-Mora, E. Gómez-Barojas, and J. A. Luna-López, "Synthesis and study of the optical properties of pmma microspheres and opals," Polymers (Basel)., vol. 13, no. 13, 2021, doi: 10.3390/polym13132171.

[115] A. Hadi, A. Hashim, and Y. Al-Khafaji, "Structural, Optical and Electrical Properties of PVA/PEO/SnO2 New Nanocomposites for Flexible Devices," Trans. Electr. Electron. Mater., vol. 21, no. 3, pp. 283–292, 2020, doi: 10.1007/s42341-020-00189-w.

[116] A. Hashim, K. H. H. Al-Attiyah, and S. F. Obaid, "Fabrication of novel (Biopolymer blend-lead oxide nanoparticles) nanocomposites: Structural and optical properties for low-cost nuclear radiation shielding," Ukr. J. Phys., vol. 64, no. 2, pp. 157–163, 2019, doi: 10.15407/ujpe64.2.157.

[117] P. P. Sahay, R. K. Nath, and S. Tewari, "Optical properties of thermally evaporated CdS thin films," Cryst. Res. Technol., vol. 42, no. 3, pp. 275–280, 2007, doi: 10.1002/crat.200610812.

[110] A. Hashim and A. Jassim, "Novel of biodegradable polymers-inorganic nanoparticles: Structural, optical and electrical properties as humidity sensors and gamma radiation shielding for biological applications," J. Bionanoscience, vol. 12, no. 2, pp. 170–176, 2018, doi: 10.1166/jbns.2018.1518.

[118] M. A. Habeeb and Z. S. Jaber, "Enhancement of Structural and Optical Properties of Cmc/Paa Blend By Addition of Zirconium Carbide Nanoparticles for Optics and Photonics Applications," East Eur. J. Phys., vol. 2022, no. 4, pp. 176–182, 2022, doi: 10.26565/2312-4334-2022-4-18.

[119] F. A. Mustafa, "Optical properties of NaI doped polyvinyl alcohol films," Arch. Pathol. Lab. Med., vol. 114, no. 12, pp. 1290–1295, 2013.

[120] S. Sabbah, M. Hasan, B. Yehiaa, and Z. Satar, "The Effect of Metal Powder on the Optical Properties of Polyvinyl Acetate," J. Adv. Res. Appl. Sci. (ISSN 2208-2352), vol. 3, no. 1, pp. 01–11, 2016, doi: 10.53555/nnas.v3i1.666.

[121] O. G. Abdullah, S. B. Aziz, K. M. Omer, and Y. M. Salih, "Reducing the optical band gap of polyvinyl alcohol (PVA) based nanocomposite," J. Mater. Sci. Mater. Electron., vol. 26, no. 7, pp. 5303–5309, 2015, doi: 10.1007/s10854-015-3067-3.

[122] Omed Gh. Abdullah; Yahya A.K. Salman; Salwan A. Saleem, "In-situ synthesis of PVA/HgS nanocomposite films and tuning optical properties," Phys. Mater. Chem., vol. 3, no. 2, pp. 18–24, 2015, doi: 10.12691/pmc-3-2-1.

[123] O. Gh Abdullah, B. K. Aziz, and S. A. Hussen, "Optical Characterization of Polyvinyl alcohol -Ammonium Nitrate Polymer Electrolytes Films," Chem. Mater. Res., vol. 3, no. 9, pp. 2225–956, 2013.

[124] A. Mohammed Kadim, A. Dheyaa Abdulkareem, A. Jawad Kadhim alrubaie, and K. Haneen Abass, "Formation of PVA-PMMA-PAAm blend with various content of dextrin for drug delivery application," Mater. Today Proc, 2021, doi: 10.1016/j.matpr.2021.06.391.

[125] O. G. Abdullah and S. A. Saleem, "Effect of Copper Sulfide Nanoparticles on the Optical and Electrical Behavior of Poly(vinyl alcohol) Films," J. Electron. Mater., vol. 45, no. 11, pp. 5910–5920, 2016, doi: 10.1007/s11664-016-4797-6.

[126] K. Rajesh, V. Crasta, N. B. R. Kumar, G. Shetty, and P. D. Rekha, "Structural , optical , mechanical and dielectric properties of titanium dioxide doped PVA / PVP nanocomposite," Journal of Polymer Research , vol. 26, no. 4, 2019, doi: 10.1007/s10965-019-1762-0.

[127] S. Mahendia, A. K. Tomar, and S. Kumar, "Electrical conductivity and dielectric spectroscopic studies of PVA-Ag nanocomposite films," J. Alloys Compd., vol. 508, no. 2, pp. 406–411, 2010, doi: 10.1016/j.jallcom.2010.08.075.

[128] Q. M. Jebur, A. Hashim, and M. A. Habeeb, "Structural, Electrical and Optical Properties for (Polyvinyl Alcohol–Polyethylene Oxide–Magnesium Oxide) Nanocomposites for Optoelectronics Applications," Trans. Electr. Electron. Mater., vol. 20, no. 4, pp. 334–343, 2019, doi: 10.1007/s42341-019-00121-x.

[129] F. T. Al-Hussein and B. H. Rabee, "Study some Electrical Properties of (PS-Tio_2-Al_2O_3) Nanocomposite Films Injected with Air Nanobubbles for Antibacterial Applications," HIV Nurs., vol. 22, no. 2, pp. 1621–1624, 2022.

[130] S. F. Obaid and R. G. Kadhim, "The effect of Ag_2O/NbO_2 nanostructures on the dielectric characteristics of PVA/PVP bled used in electronics," J. Phys. Conf. Ser., vol. 2322, no. 1, 2022, doi: 10.1088/1742-6596/2322/1/012080.

[131] A. Hashim and Z. S. Hamad, "The activity levels of Lactate dehydrogenase in the seminal plasma of normospermic and infertile men," Adv. Nat. Appl. Sci., vol. 12, no. 10, pp. 12–16, 2018, doi: 10.22587/anas.2018.12.10.2.

[132] A. Hashim and Z. S. Hamad, "Antibacterial Activity of Biopolymer Blend-Carbide Nanoparticles Bio-Films against Escherichia Coli," Res. J. Agric. Biol. Sci., no. September, 2018, doi: 10.22587/rjabs.2018.13.2.1.

[133] R. M. Mohammed, "Effect of Antimony Oxide Nanoparticles on Structural, Optical and AC Electrical Properties of (PEO-PVA) Blend for Antibacterial Applications," Int. J. Emerg. Trends Eng. Res., vol. 8, no. 8, pp. 4726–4738, 2020, doi: 10.30534/ijeter/2020/107882020.

[134] Z. S. Jaber and M. A. Habeeb, "Structural and Dielectrically Properties of (CMC -PAA-ZrC) Nano Composites for Gamma Shielding Application," vol. 44, no. 8, pp. 371–377, 2021.

[135] H. H. Jassim and F. S. Hashim, "Synthesis of (Pva/peg: Zno and co3o4) nanocomposites: Characterization and gamma ray studies," NeuroQuantology, vol. 19, no. 4, pp. 47–56, 2021, doi: 10.14704/nq.2021.19.4.NQ21036.

الخلاصة

تم تحضير المركبات النانوية (بولي مثيل ميثاكريلات - بولي اثيلين كلايكول /نتريد السيلكون) بطريقة الصب بتراكيز مختلفة من جسيمات نتريد السيلكون النانوية. الخصائص التركيبية التي تمت دراستها والتي تشمل المجهر البصري(OM) ، والمجهر الإلكتروني الماسح (SEM) ، وتحويل فوربيه للأشعة تحت الحمراء FT-IR تمت دراسة الخصائص البصرية والكهربائية للمركبات النانوية, أظهرت صور الفحص المجهري الضوئي أنه مع زيادة تركيزات الجسيمات النانوية، تتشكل مسارات الشبكة داخل المصفوفة البوليمرية التي تعمل كحاملات شحنة. وأظهرت نتائج قياس SEM توزيعًا جيدًا ومتجانسًا في مورفولوجيا السطح. تشير نتائج FT-IR إلى تداخل مادي بين وسط البوليمر والجسيمات النانوية. بينما أظهرت نتائج الخصائص البصرية للمركبات النانوية (PMMA-PEG/Si_3N_4) أن الامتصاص ومعامل الامتصاص ومعامل الخمود ومعامل الانكسار وثوابت العزل الكهربائية الحقيقية والخيالية وكذلك التوصيلية البصرية تزداد مع زيادة تركيزات الجسيمات النانويةSi_3N_4 ، بينما تنخفض فجوة الطاقة مع زيادة تركيز الجسيمات النانوية كما أشارت إلى أن أعلى امتصاص للطيف حدث في منطقة U.V. . أظهرت نتائج الخصائص الكهربائية للمركبات النانوية أن ثابت العزل الكهربائي وفقدان العزل الكهربائي يزدادان مع زيادة تركيز الجسيمات النانوية وينخفضان مع زيادة تردد المجال الكهربائي المطبق. بينما تزداد الموصلية الكهربائية A.Cمع زيادة تردد وتركيز (Si_3N_4). أظهرت نتائج تطبيقات (PMMA-PEG/Si_3N_4) المركبات النانوية ضد البكتيريا أن منطقة قطر التثبيط تزداد مع زيادة تركيزات الجسيمات النانوية، وتزداد معاملات التوهين لأشعة كاما مع زيادة تركيزات الجسيمات النانوية.

جمهورية العراق
وزارة التعليم العالي والبحث العلمي
جامعة بابل
كلية التربية للعلوم الصرفة
قسـم الفـيزياء

تأثير نتريد السيلكون النانوي على الخصائص التركيبية ، البصرية والكهربائية لخليط بوليمري وتطبيقاته

رسالة مقدمة
إلى مجلس كلية التربية للعلوم الصرفة في جامعة بابل كجزء من متطلبات
نيل درجة الماجستير في التربية / الفيزياء

من قبل الطالب

غيث احمد عبد الله مراد

بكالوريوس تربية فيزياء

جامعة بابل 2020 م

بإشراف

أ.د. احمد هاشم محيسن

2023 م 1444 هـ